8

Cosine Modulated Filter Banks

8.0 INTRODUCTION

In Chap. 5 and 6 we considered M channel maximally decimated analysis/synthesis systems, and studied various errors, as well as techniques to eliminate these. In particular, we studied the concept of perfect reconstruction (PR) in detail, and presented techniques to design FIR PR systems.

In this Chapter we will present filter banks based on cosine modulation. In these systems, all the M analysis filters are derived from a prototype filter $P_0(z)$ by cosine modulation. Two outstanding advantages of these systems are:

1. The cost of the analysis bank is equal to that of one filter, plus modulation overhead. The modulation itself can be done by fast techniques such as the fast discrete cosine transform (DCT). See, for example, Yip and Rao [1987]. The synthesis filters have the same cost as the analysis filters.
2. During the design phase, where we optimize the filter coefficients, the number of parameters to be optimized is very small because only the prototype has to be optimized.

Two classes of such systems will be studied — approximate reconstruction systems (pseudo QMF) and perfect reconstruction systems.

A. Cosine Modulated Pseudo QMF Banks (Sec. 8.1–8.3)

Prior to the development of perfect reconstruction systems, several authors have developed techniques for designing *approximate reconstruction* systems. These are called the pseudo QMF systems, introduced by Nussbaumer [1981] and developed further by Rothweiler [1983], Chu [1985], Masson and Picel [1985j, and Cox [1986]. In these systems the analysis and synthesis filters $H_k(z)$ and $F_k(z)$ are chosen so that only "adjacent-channel aliasing" (to be explained below) is canceled, and the distortion function

$T(z)$ is only approximately a delay. Such approximate systems, called *pseudo* QMF banks, are acceptable in some practical applications.

B. Cosine Modulated Perfect Reconstruction Systems (Sec. 8.5)

More recently, cosine modulated systems with the perfect reconstruction property have been developed independently by Malvar [1990b and 1991], Ramstad [1991], and Koilpillai and Vaidyanathan [1991a and 1992]. These are paraunitary systems. They retain all the simplicity and economy of the pseudo QMF system, and yet have the perfect reconstruction property. In Sec. 8.4 we study some properties of cosine modulation matrices. These are then used in Sec. 8.5 to derive cosine modulated perfect reconstruction systems. *These two sections can be studied independently of the pseudo QMF derivations, with Sections 8.1–8.3 serving only as references.*

8.1 THE PSEUDO QMF BANK

In this section we present the theory of pseudo QMF banks. In Sec. 8.2 and 8.3 we will outline design procedures and structures for these. Readers interested only in perfect reconstruction systems can go directly to Sec. 8.4 (and use sections 8.1–8.3 only as a reference).

8.1.1 Generation of M Real Coefficient Analysis Filters

In Sec. 4.3.2 we saw how a set of M filters can be derived from one prototype filter by use of the structure of Fig. 4.3-5(a). In that structure, the filters $E_\ell(z)$ represent the Type 1 polyphase components of the prototype filter $H_0(z)$, and the filters $H_k(z)$ are related to $H_0(z)$ as $H_k(z) = H_0(zW_M^k)$, where $W_M = e^{-j2\pi/M}$. This means that the frequency responses $H_k(e^{j\omega})$ are uniformly shifted versions of the prototype, as demonstrated in Fig. 4.3-5(b). Since $h_k(n)$ is obtained by exponential modulation of $h_0(n)$, (that is, $h_k(n) = h_0(n)e^{j2\pi kn/M}$), the coefficients $h_k(n)$ are in general complex even if $h_0(n)$ is real. This means that the output of $H_k(z)$ could be a complex signal even if the input $x(n)$ is real.

We now derive a class of filters with real coefficients, by using *cosine* modulation rather than exponential modulation. This can be done by first obtaining $2M$ complex filters using exponential modulation, and then combining appropriate pairs of filters.

Consider Fig. 8.1-1 which is a modification of Fig. 4.3-5(a) (replace M with $2M$). This is a uniform-DFT analysis bank, with the $2M$ filters related as

$$P_k(z) = P_0(zW^k), \quad \text{that is,} \quad p_k(n) = p_0(n)W^{-kn}. \tag{8.1.1}$$

In this section, unsubscripted W stands for W_{2M}, that is,

$$W = W_{2M} = e^{-j2\pi/2M} = e^{-j\pi/M}. \tag{8.1.2}$$

Also, $\mathbf{W}$ is the $2M \times 2M$ DFT matrix.

$P_0(z)$ is called the prototype filter. Throughout this chapter, its impulse response $p_0(n)$ is real so that $|P_0(e^{j\omega})|$ is symmetric with respect to $\omega = 0$. This filter is typically lowpass, with cutoff frequency $\pi/2M$ [Fig. 8.1-2(a)]. The polyphase components of $P_0(z)$ are $G_k(z), 0 \leq k \leq 2M-1$.

From (8.1.1) we have

$$P_k(e^{j\omega}) = P_0\left(e^{j(\omega - \frac{k\pi}{M})}\right), \tag{8.1.3}$$

that is, the response $P_k(e^{j\omega})$ is the right-shifted version of $P_0(e^{j\omega})$ by an amount $k\pi/M$ [Fig. 8.1-2(b)]. From the figure we see that the responses $|P_k(e^{j\omega})|$ and $|P_{2M-k}(e^{j\omega})|$ are images of each other with respect to zero-frequency, so that they are suitable candidates to be combined, to get a real coefficient filter. The typical passband width of such a 'combined filter' is equal to $2\pi/M$, which is twice that of $P_0(z)$ (which is not combined with any other filter).

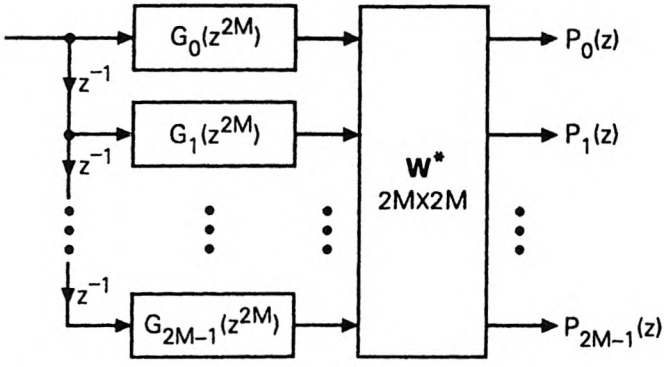

Figure 8.1-1 Generation of $2M$ uniformly shifted filters from prototype $P_0(z)$. Here $G_m(z)$, $0 \leq m \leq 2M-1$, are the polyphase components of $P_0(z)$.

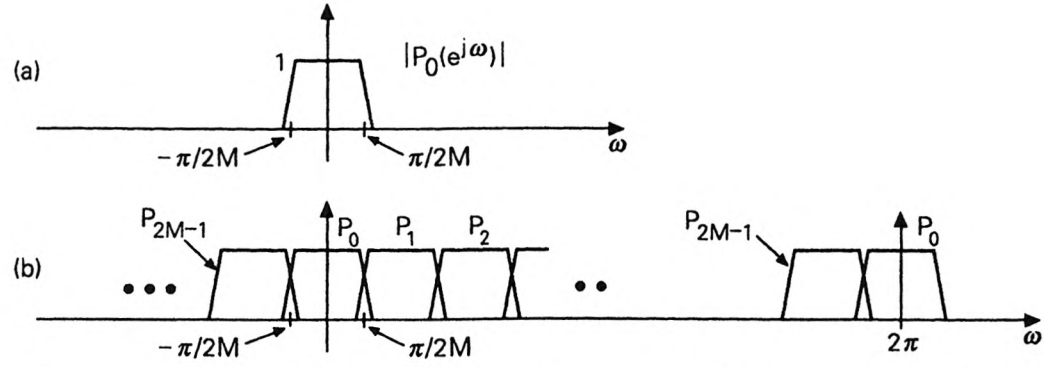

Figure 8.1-2 (a) Magnitude response of the prototype $P_0(z)$, and (b) Magnitude responses of shifted versions.

In order to make all the filter bandwidths equal after combining pairs, we use a *right-shifted version* of the original set of $2M$ responses [Fig. 8.1-3(a)], the amount of right-shift being $\pi/2M$. This is accomplished by replacing z with $zW^{0.5}$ as indicated in Fig. 8.1-3(b). (The quantity z^{2M} is replaced with $-z^{2M}$ since $W^M = W_{2M}^M = -1$.) The complex filters $Q_k(z)$ are given in terms of the prototype $P_0(z)$ by

$$Q_k(z) = P_0(zW^{k+0.5}), \quad 0 \le k \le 2M-1. \tag{8.1.4}$$

The magnitude responses of $Q_k(z)$ and $Q_{2M-1-k}(z)$ are now images of each other with respect to zero-frequency, that is, $|Q_k(e^{j\omega})| = |Q_{2M-1-k}(e^{-j\omega})|$. The impulse response coefficients of $Q_k(z)$ and $Q_{2M-1-k}(z)$ are conjugates of each other, that is,

$$Q_{2M-1-k}(z) = Q_{k,*}(z)$$

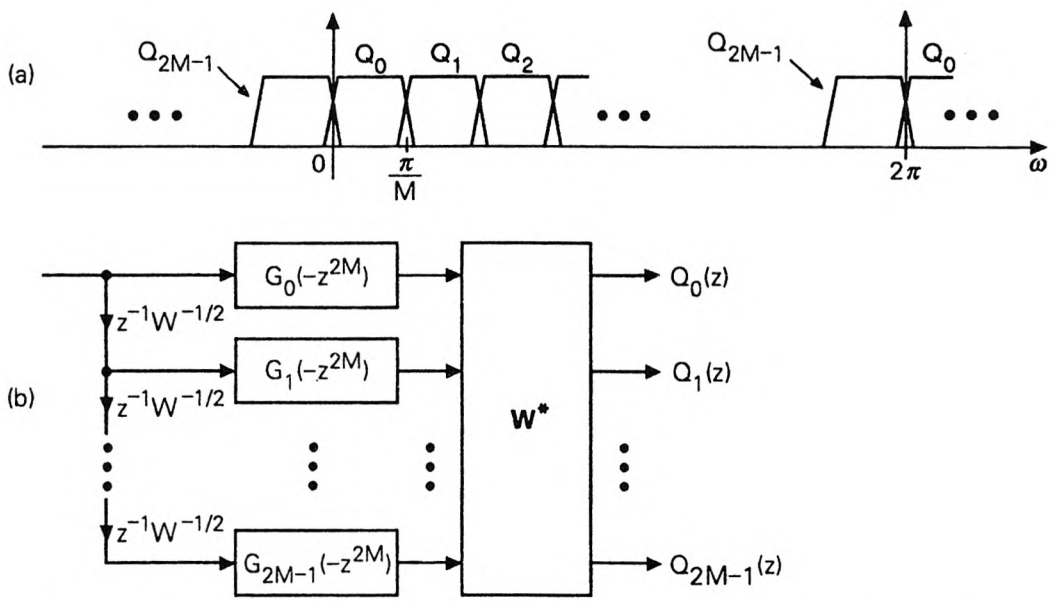

Figure 8.1-3 Shifting the responses by $\pi/2M$, by replacing z with $zW^{1/2}$.

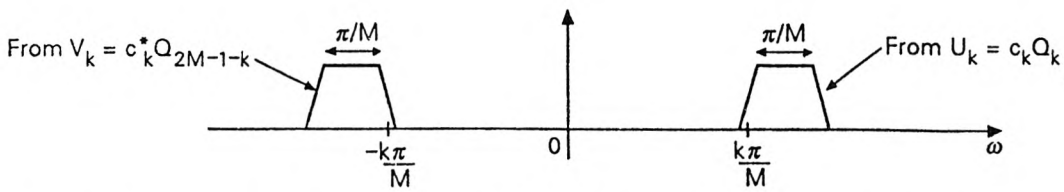

Figure 8.1-4 Magnitude response of the kth analysis filter $H_k(z)$. Synthesis filter $F_k(z)$ is chosen to have similar magnitude response. See text.

Definition of the Real Coefficient Analysis Filters

Define

$$U_k(z) = c_k P_0(zW^{k+0.5}) = c_k Q_k(z) \tag{8.1.5}$$

and

$$V_k(z) = c_k^* P_0(zW^{-(k+0.5)}) = c_k^* Q_{2M-1-k}(z). \tag{8.1.6}$$

We then generate the M analysis filters as follows:

$$H_k(z) = a_k U_k(z) + a_k^* V_k(z), \quad 0 \le k \le M-1. \tag{8.1.7}$$

Here c_k and a_k are unit-magnitude constants, whose purpose will be clarified soon. (Actually, we could have done away with c_k by absorbing it in a_k, but the above form is more convenient for discussion.) Fig. 8.1-4 summarizes the situation.

We will assume the prototype to be of the form

$$P_0(z) = \sum_{n=0}^{N} p_0(n) z^{-n}, \tag{8.1.8}$$

that is, Nth order FIR. All analysis filters are then FIR with order $\le N$, that is,

$$H_k(z) = \sum_{n=0}^{N} h_k(n) z^{-n}, \quad 0 \le k \le M-1. \tag{8.1.9}$$

Since the coefficients of $P_0(z)$ are real, the coefficients of $V_k(z)$ and $U_k(z)$ are conjugates of each other. So $h_k(n)$ are real.

8.1.2 Alias Cancelation

Recall the intricacies of alias cancelation (Sec. 5.4.2). The decimated output of $H_k(z)$ gives rise to the alias components $H_k(zW_M^\ell)X(zW_M^\ell)$, [i.e., frequency-shifted versions of $H_k(z)X(z)$]. The synthesis filter $F_k(z)$, whose passband coincides with that of $H_k(z)$, retains the unshifted version $H_k(z)X(z)$, and also permits a small leakage of the shifted versions. When we add the outputs of all M synthesis filters, these leakages should "somehow" be canceled.

Remembering that the passbands of $F_k(z)$ should coincide with those of $H_k(z)$, we generate $F_k(z)$ as

$$F_k(z) = b_k U_k(z) + b_k^* V_k(z), \quad 0 \le k \le M-1, \tag{8.1.10}$$

where b_k are unit-magnitude constants. (The choice of a_k, b_k and c_k will soon be settled.)

In general, the output of $F_k(z)$ has the components $H_k(zW_M^\ell)X(zW_M^\ell)$ for all values of ℓ, i.e., $0 \le \ell \le M-1$. However, if the stopband attenuation

of $F_k(z)$ is sufficiently high, only some of these components are of practical significance. The other components, though not exactly equal to zero, will be ignored, giving rise to the term "approximate alias cancelation."

Figure 8.1-5 shows some of the shifted versions $U_k(zW_M^{\ell})$ and $V_k(zW_M^{\ell})$. Notice that, the response of $U_k(zW_M)$ does *not* overlap with that of $U_k(z)$. However, the responses of $U_k(zW_M^{-k})$ and $U_k(zW_M^{-(k+1)})$ overlap with the response of $V_k(z)$. Similarly, the responses of $V_k(zW_M^{k})$ and $V_k(zW_M^{(k+1)})$ have overlap with that of $U_k(z)$. This means that the alias-components $X(zW_M^{\ell})$, which are significant at the output of $F_k(z)$, correspond to

$$\ell = -(k+1), -k, k, k+1 \qquad [\text{output of } F_k(z)] \tag{8.1.11}$$

Similarly, at the output of $F_{k-1}(z)$, the significant alias components are for

$$\ell = -k, -(k-1), (k-1), k \qquad [\text{output of } F_{k-1}(z)]. \tag{8.1.12}$$

Note that negative values of ℓ should be interpreted modulo M. For example, $\ell = -1$ is equivalent to $\ell = M - 1$.

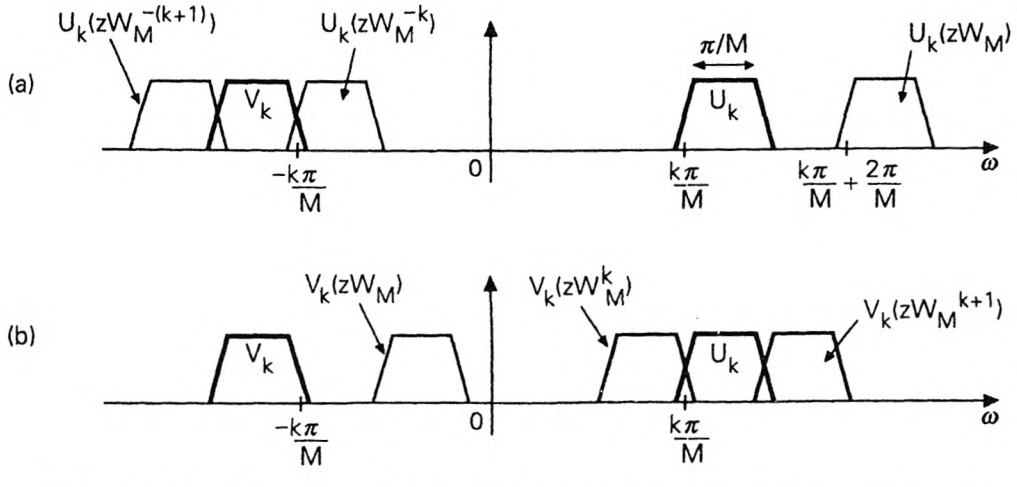

Figure 8.1-5 Demonstration of alias components which overlap with main synthesis filter response $|F_k(e^{j\omega})|$.

Constraint on a_k and b_k to Cancel Aliasing

Here, then, is the fundamental principle behind the approximate alias cancelation scheme: since the outputs of $F_k(z)$ as well as $F_{k-1}(z)$ have the common alias components $X(zW_M^{\pm k})$, we try to choose $F_{k-1}(z)$ and $F_k(z)$ such that this component is canceled when these outputs are added. In fact, such cancelation can be accomplished just by appropriately constraining a_k and b_k, as we show next.

The negative-frequency part of $F_k(z)$, [i.e., $b_k^* V_k(z)$] has the following significant alias components:

$$\begin{aligned}&\Big(a_k b_k^* U_k(zW_M^{-k})V_k(z)\Big)X(zW_M^{-k})\\&+\Big(a_k b_k^* U_k(zW_M^{-(k+1)})V_k(z)\Big)X(zW_M^{-(k+1)}),\end{aligned}\tag{8.1.13}$$

and the negative-frequency part of $F_{k-1}(z)$ has

$$\begin{aligned}&\Big(a_{k-1} b_{k-1}^* U_{k-1}(zW_M^{-(k-1)})V_{k-1}(z)\Big)X(zW_M^{-(k-1)})\\&+\Big(a_{k-1} b_{k-1}^* U_{k-1}(zW_M^{-k})V_{k-1}(z)\Big)X(zW_M^{-k}).\end{aligned}\tag{8.1.14}$$

The alias component $X(zW_M^{-k})$ can therefore be eliminated if

$$a_k b_k^* U_k(zW_M^{-k})V_k(z) + a_{k-1} b_{k-1}^* U_{k-1}(zW_M^{-k})V_{k-1}(z) = 0. \tag{8.1.15}$$

By using the definitions for $U_k(z)$ and $V_k(z)$, and the condition $|c_k| = |c_{k-1}| = 1$, we can rewrite (8.1.15) entirely in terms of $V_i(z)$'s as

$$(a_k b_k^* + a_{k-1} b_{k-1}^*)V_{k-1}(z)V_k(z) = 0. \tag{8.1.16}$$

This condition can be satisfied by constraining a_i and b_i such that

$$a_k b_k^* = -a_{k-1} b_{k-1}^*, \quad 1 \le k \le M-1. \tag{8.1.17}$$

By considering the signal at the output of the positive frequency component $b_k U_k(z)$ of $F_k(z)$, we again obtain the same condition for alias cancelation. More specific choice of a_k and b_k will be given soon.

8.1.3 Eliminating Phase Distortion

Having canceled aliasing, we now turn to the distortion function $T(z)$. From Sec. 5.4.2 we know that $T(z)$ can always be expressed as

$$T(z) = \frac{1}{M}\sum_{k=0}^{M-1} F_k(z)H_k(z). \tag{8.1.18}$$

The QMF bank is free from phase distortion if $T(z)$ has linear phase. We can ensure this if the synthesis filters are chosen according to the mirror image condition

$$f_k(n) = h_k(N-n), \tag{8.1.19a}$$

or equivalently as

$$F_k(z) = z^{-N}H_k(z^{-1}) = z^{-N}\widetilde{H}_k(z) \qquad (\text{as } h_k(n) \text{ is real}). \tag{8.1.19b}$$

In this case (8.1.18) becomes

$$T(z) = \frac{z^{-N}}{M} \sum_{k=0}^{M-1} H_k(z^{-1}) H_k(z). \tag{8.1.20}$$

Clearly

$$MT(e^{j\omega}) = e^{-j\omega N} \sum_{k=0}^{M-1} |H_k(e^{j\omega})|^2, \tag{8.1.21}$$

which shows that $T(z)$ has linear phase.

We know that $H_k(z)$ and $F_k(z)$ are already related in some way because of their definitions in terms of the same set of components $U_k(z)$ and $V_k(z)$. By careful choice of the constants a_k, b_k, c_k, we can satisfy the additional relation (8.1.19) as well. We do this in two steps as follows.

Choice of c_k to Ensure Linear Phase of $U_k(z)$ and $V_k(z)$

The phase response of $P_0(z)$ has not entered our discussion so far. We will now restrict $P_0(z)$ to be a linear phase filter with symmetric $p_0(n)$, that is, $p_0(n) = p_0(N - n)$, so that

$$\widetilde{P}_0(z) = z^N P_0(z). \tag{8.1.22}$$

[Antisymmetric $p_0(n)$ would be inconsistent, since $P_0(z)$ is lowpass.] We then have

$$P_0(e^{j\omega}) = e^{-j\omega N/2} P_R(\omega), \tag{8.1.23}$$

where $P_R(\omega)$ is real-valued (Sec. 2.4.2). We will choose c_k so that the complex-coefficient filters $U_k(z)$ and $V_k(z)$ have same (linear) phase as $P_0(z)$. (This will make it easier to determine the appropriate choice of a_k and b_k later.) From (8.1.5) we have

$$U_k(e^{j\omega}) = c_k W^{-(k+0.5)N/2} e^{-j\omega N/2} P_R\Big(\omega - \frac{\pi(k+0.5)}{M}\Big). \tag{8.1.24}$$

If we choose

$$c_k = W^{(k+0.5)N/2}, \tag{8.1.25}$$

then

$$U_k(e^{j\omega}) = e^{-j\omega N/2} P_R\left(\omega - \frac{\pi(k+0.5)}{M}\right). \tag{8.1.26}$$

Since $P_R(\omega)$ is real, $U_k(z)$ is a linear phase filter with phase response $\phi(\omega) = -\omega N/2$. Thus the phase responses of the modulated filters $U_k(z)$ are identical to that of the prototype $P_0(e^{j\omega})$. Same is true of $V_k(z)$, with c_k chosen as above.

Choice of b_k to Ensure the Relation $F_k(z) = z^{-N}H_k(z^{-1})$

The linear phase nature of $U_k(z)$ and $V_k(z)$ permits us to write

$$\widetilde{U}_k(z) = z^N U_k(z), \quad \widetilde{V}_k(z) = z^N V_k(z), \tag{8.1.27}$$

analogous to (8.1.22). By using these relations in (8.1.7) we can verify

$$z^{-N}\widetilde{H}_k(z) = a_k^* U_k(z) + a_k V_k(z). \tag{8.1.28}$$

If we now choose

$$b_k = a_k^*, \tag{8.1.29}$$

then the RHS of (8.1.28) reduces to $F_k(z)$ [defined as in (8.1.10)]. This proves that the mirror image condition (8.1.19b) can indeed be satisfied by enforcing the constraint $b_k = a_k^*$. The distortion $T(z)$ now takes the form (8.1.20), and hence has linear phase.

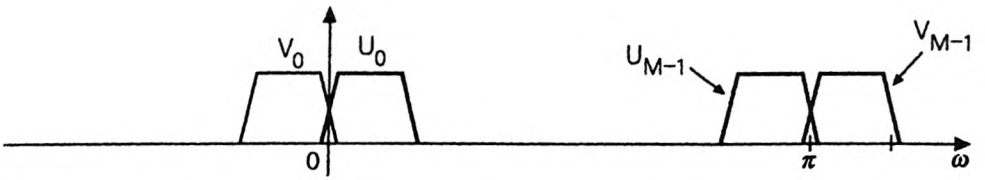

Figure 8.1-6 Demonstration of overlap of $V_0(e^{j\omega})$ with $U_0(e^{j\omega})$, and overlap of $V_{M-1}(e^{j\omega})$ with $U_{M-1}(e^{j\omega})$.

Choice of a_k

It only remains to choose a_k. The alias cancelation constraint (8.1.17) can be simplified by using the further relation (8.1.29) to obtain $a_k^2 = -a_{k-1}^2$, that is,

$$a_k = \pm j a_{k-1}. \tag{8.1.30}$$

This can be used to determine all a_k's, provided a_0 is somehow determined. To make this final choice, we note that the components $U_k(z)$ and $V_k(z)$ do not overlap significantly except when $k = 0$ or $M-1$ (Fig. 8.1-6). So the expression (8.1.18) can be simplified into

$$\begin{aligned} MT(z) \approx\ & (a_0^2 + a^{*2}_0)U_0(z)V_0(z) \\ & + (a_{M-1}^2 + a^{*2}_{M-1})U_{M-1}(z)V_{M-1}(z) \\ & + \sum_{k=0}^{M-1} \Big(U_k^2(z) + V_k^2(z)\Big), \end{aligned} \tag{8.1.31}$$

by using the condition $a_k b_k = a_k a_k^* = 1$. The cross-terms $U_0(z)V_0(z)$ and $U_{M-1}(z)V_{M-1}(z)$ can create significant distortions around the frequencies $\omega = 0$ and $\omega = \pi$, respectively. By constraining a_0 and a_{M-1} such that

$$a_0^4 = a_{M-1}^4 = -1, \tag{8.1.32}$$

we can eliminate these cross-terms, yielding

$$T(z) \approx \frac{1}{M} \sum_{k=0}^{M-1} \Big(U_k^2(z) + V_k^2(z) \Big). \tag{8.1.33}$$

Based on these considerations we choose

$$a_k = e^{j\theta_k}, \quad \theta_k = (-1)^k \frac{\pi}{4}, \quad 0 \le k \le M-1. \tag{8.1.34}$$

This implies $a_k = (-1)^k j a_{k-1}$, satisfying (8.1.30). Evidently (8.1.32) is also satisfied. We also choose b_k and c_k as stated above. All constants are now determined.

Summary

1. The condition for alias cancelation is given by $a_k b_k^* = -a_{k-1} b_{k-1}^*$.
2. The choice $c_k = W^{(k+0.5)N/2}$ (where $W = e^{-j\pi/M}$) ensures that $U_k(z)$ and $V_k(z)$ have the same (linear) phase response as the propotype $P_0(z)$. (This is a convenience which simplifies further design rules.)
3. The further constraint $b_k = a_k^*$ forces the relation $F_k(z) = z^{-N} H_k(z^{-1})$. This in turn leads to the linear phase form (8.1.20) for $T(z)$.
4. The constraint $a_k = (-1)^k j a_{k-1}$, together with $b_k = a_k^*$ ensures that the above alias cancelation condition is satisfied. Consistent with this constraint on a_k, we choose $a_k = e^{j\theta_k}$, $\theta_k = (-1)^k \pi/4$. This also ensures (8.1.32) so that $T(z)$ is further simplified to (8.1.33) (i.e., the two cross-terms given by $U_0(z)V_0(z)$ and $U_{M-1}(z)V_{M-1}(z)$, which can cause amplitude distortion around $\omega = 0$ and π, are eliminated).
5. Summarizing, the M analysis filters are given by (8.1.37) (see below), with $\theta_k = (-1)^k \pi/4$. With the synthesis filters chosen as in (8.1.19a), we have approximate alias cancelation and complete elimination of phase distortion. Amplitude distortion still remains, and should be minimized as shown in the next section. Notice finally that all the analysis and synthesis filters have real coefficients.

8.1.4 Closed Form Expressions for the Filters

We now find expressions for the analysis filters $h_k(n)$. The first term in (8.1.7) is

$$\begin{aligned} a_k U_k(z) &= e^{j\theta_k} c_k P_0(zW^{k+0.5}) \\ &= e^{j\theta_k} W^{(k+0.5)N/2} \sum_{n=0}^{N} p_0(n) W^{-(k+0.5)n} z^{-n}, \end{aligned} \tag{8.1.35}$$

so that its impulse response coefficients are

$$e^{j\theta_k} W^{(k+0.5)N/2} p_0(n) W^{-(k+0.5)n}. \tag{8.1.36}$$

The coefficients of the second term in (8.1.7) are obtained by conjugating this. So $h_k(n)$ equals two times the real part of the first term, that is,

$$h_k(n) = 2p_0(n)\cos\Big(\frac{\pi}{M}(k+0.5)(n-\frac{N}{2}) + \theta_k\Big), \tag{8.1.37}$$

(since $p_0(n)$ is real). The synthesis filters $f_k(n)$ are obtained by replacing a_k with b_k. Since $b_k = a_k^*$, this is equivalent to replacing θ_k with $-\theta_k$, that is,

$$f_k(n) = 2p_0(n)\cos\Big(\frac{\pi}{M}(k+0.5)(n-\frac{N}{2}) - \theta_k\Big). \tag{8.1.38}$$

We can obtain this same $f_k(n)$ by using the mirror image relation (8.1.19), which we imposed in the above derivation. The analysis and synthesis filters, in general, do not have linear phase (even though the prototype $P_0(z)$ has linear phase). The distortion function $T(z)$, however, has linear phase.

As all the analysis and synthesis filters are related to the prototype $p_0(n)$ by cosine modulation, the only design freedom for the QMF bank is in the choice of $p_0(n)$. This design issue will be addressed in the next section.

8.2 DESIGN OF THE PSEUDO QMF BANK

In the previous section we considered the pseudo QMF bank, and eliminated phase distortion and (approximately) eliminated aliasing. It only remains to reduce amplitude distortion. Recall that amplitude distortion arises if $|T(e^{j\omega})|$ is not exactly flat. The prototype $P_0(z)$ should now be designed in such a way that $|T(e^{j\omega})|$ is acceptably flat.

8.2.1 Reducing Amplitude Distortion

We begin by pointing out some subtleties about the behavior of the distortion function $T(z)$.

Unit-Circle Zeros of T(z)

We know that it is undesirable for $T(z)$ to have zeros on the unit circle, as this would imply severe amplitude distortion. From the expression (8.1.21) we see that $T(e^{j\omega_0})$ is nonzero unless all the M filters satisfy $H_k(e^{j\omega_0}) = 0$. This unfortunate situation will not arise, unless the passband width of the prototpe $P_0(e^{j\omega})$ is unreasonably narrow.

Periodicity of $|T(e^{j\omega})|$

Consider the linear phase prototype (8.1.23). From Sec. 2.4.2 we know that $P_R^2(\omega)$ has period 2π for any N. Define $F(e^{j\omega}) = P_R^2(\omega)$ and $G(z) = F(zW^{0.5})$. We can then express (8.1.33) as

$$T(z) \approx \frac{z^{-N}}{M}\sum_{k=0}^{2M-1} G(zW^k), \tag{8.2.1}$$

by using the simplified expression for $U_k(z)$ [i.e. eqn. (8.1.26)] and the fact that $v_k(n) = u_k^*(n)$. With $G(z) = \sum g(n)z^{-n}$, the summation in the above equation simplifies to

$$\sum_{k=0}^{2M-1} G(zW^k) = \sum_n g(n)z^{-n} \sum_{k=0}^{2M-1} W^{-kn} = 2M \sum_n g(2Mn)z^{-2Mn}, \tag{8.2.2}$$

showing that the variable z appears only in powers such as z^{2M}. This shows that $T(z)$ has the form

$$T(z) \approx z^{-N} f(z^{2M}), \tag{8.2.3}$$

for some FIR $f(z)$. In particular, therefore, $|T(e^{j\omega})|$ has period $2\pi/2M$.

Origin of Amplitude Distortion

Consider the expression (8.1.33). If ω is a frequency belonging to passband of some filter $U_k(z)$, then $T(e^{j\omega}) \approx U_k^2(e^{j\omega})/M$. This shows that $|T(e^{j\omega})|$ is nearly the same at all frequencies which belong to the passbands of $U_k(z)$'s (or $V_k(z)$'s). However, if ω is at the transition between $U_k(e^{j\omega})$ and $U_{k+1}(e^{j\omega})$ [see Fig. 8.2-1(a)], then

$$T(e^{j\omega}) \approx \frac{1}{M}\left(U_k^2(e^{j\omega}) + U_{k+1}^2(e^{j\omega})\right). \tag{8.2.4}$$

Substituting from (8.1.26), this reduces to

$$\frac{e^{-j\omega N}}{M}\left(\left|P_0(e^{j(\omega - \frac{k\pi}{M} - \frac{\pi}{2M})})\right|^2 + \left|P_0(e^{j(\omega - \frac{(k+1)\pi}{M} - \frac{\pi}{2M})})\right|^2\right). \tag{8.2.5}$$

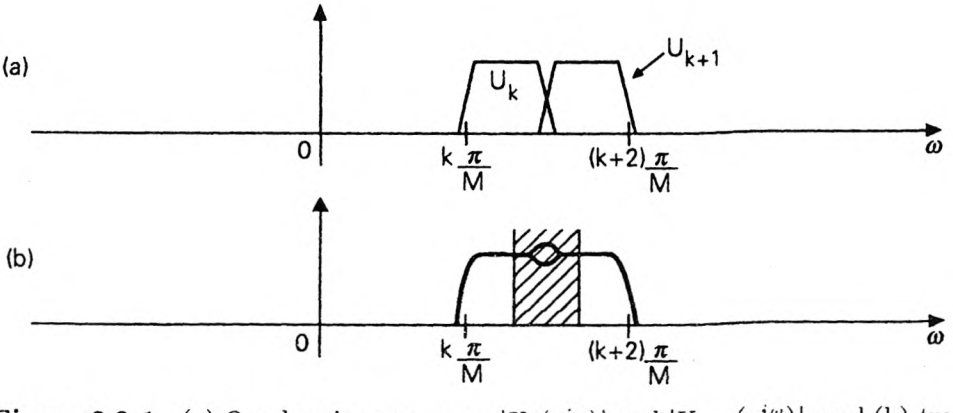

Figure 8.2-1 (a) Overlapping responses $|U_k(e^{j\omega})|$ and $|U_{k+1}(e^{j\omega})|$, and (b) two possible behaviors of $|U_k^2(e^{j\omega}) + U_{k+1}^2(e^{j\omega})|$, explaining the origin of amplitude to distortion.

Typical behaviors of this quantity are illustrated in Fig. 8.2-1(b). Assuming the prototype $P_0(z)$ to have 'good' stopband attenuation, this quantity is significant only in the frequency interval

$$\frac{k\pi}{M} \leq \omega \leq \frac{(k+2)\pi}{M}.$$

It can exhibit a 'bump' or 'dip' around the transition frequency $(k+1)\pi/M$. This is the source of amplitude distortion, that is, nonflatness of $|T(e^{j\omega})|$.

An Objective Function Representing the Flatness Requirement

Notice that the quantity in paranthesis in (8.2.5) is nothing but a frequency-shifted version of

$$|P_0(e^{j\omega})|^2 + |P_0(e^{j(\omega-\frac{\pi}{M})})|^2. \tag{8.2.6}$$

It follows that if we force this to be sufficiently 'flat,' then $|T(e^{j\omega})|$ will be "sufficiently flat" for all frequencies. This can be accomplished during the design of the prototype $p_0(n)$ by including a term in the objective function, to reflect the nonflatness of (8.2.6). Such an objective function is given by

$$\phi_1 = \int_0^{\pi/M} \left(|P_0(e^{j\omega})|^2 + |P_0(e^{j(\omega-\frac{\pi}{M})})|^2 - 1\right)^2 d\omega. \tag{8.2.7}$$

The above limits of integration are justified because $|T(e^{j\omega})|$ has period π/M as shown above.

8.2.2 Design of the Prototype Filter

The prototype $P_0(z)$ is a real coefficient linear phase FIR lowpass filter with cutoff $\pi/2M$ [Fig. 8.1-2(a)]. By designing it to have good stopband attenuation, we improve the attenuation characteristics of all the filters $H_k(z)$ and $F_k(z)$. Our choice of constants a_k, b_k, c_k above already ensures that aliasing and phase distortion are eliminated. By designing $P_0(z)$ such that (8.2.7) is small, one can reduce the amplitude distortion as well.

An appropriate measure of stopband attenuation of $P_0(z)$ is given by

$$\phi_2 = \int_{\frac{\pi}{2M}+\epsilon}^{\pi} |P_0(e^{j\omega})|^2 d\omega. \tag{8.2.8}$$

(The choice of $\epsilon > 0$ depends on the acceptable transition bandwidth.) So we optimize the coefficients $p_0(n)$ of $P_0(z)$ to minimize

$$\phi = \alpha\phi_1 + (1-\alpha)\phi_2 \quad \text{(composite objective function)}, \tag{8.2.9}$$

where α is a tradeoff parameter with $0 < \alpha < 1$. Standard nonlinear optimization packages [Press, et al, 1989] can be used for this.

TABLE 8.2.1 Design example 8.2.1. Impulse response of the FIR prorotype filter for pseudo QMF design.

n	$p_0(n)$
0	−2.9592103 e−03
1	−4.0188527 e−03
2	−4.9104756 e−03
3	−5.4331753 e−03
4	−5.3730961 e−03
5	−4.5222385 e−03
6	−2.6990818 e−03
7	2.3096829 e−04
8	4.3373153 e−03
9	9.6099830 e−03
10	1.5951440 e−02
11	2.3175400 e−02
12	3.1013020 e−02
13	3.9127130 e−02
14	4.7132594 e−02
15	5.4622061 e−02
16	6.1194772 e−02
17	6.6485873 e−02
18	7.0193888 e−02
19	7.2103807 e−02

Design example 8.2.1: Pseudo QMF Bank

We now show details of an 8-channel system ($M = 8$), with prototype filter order $N = 39$. The coefficients of the prototye $P_0(z)$, designed as described above, are shown in Table 8.2.1. (Only the first half is shown due to linear phase). Fig. 8.2-2 shows the prototype magnitude response $|P_0(e^{j\omega})|$, whereas Fig. 8.2-3 shows the magnitude responses of the analysis filters. Adjacent filter responses intersect approximately at the 3 dB level. This is consistent with the expression

$$|T(e^{j\omega})| = \frac{1}{M} \sum_{k=0}^{M-1} |H_k(e^{j\omega})|^2,$$

because, at the transition between two filters, only two of the M terms in the above summation are significant, and these are required to add up to unity.

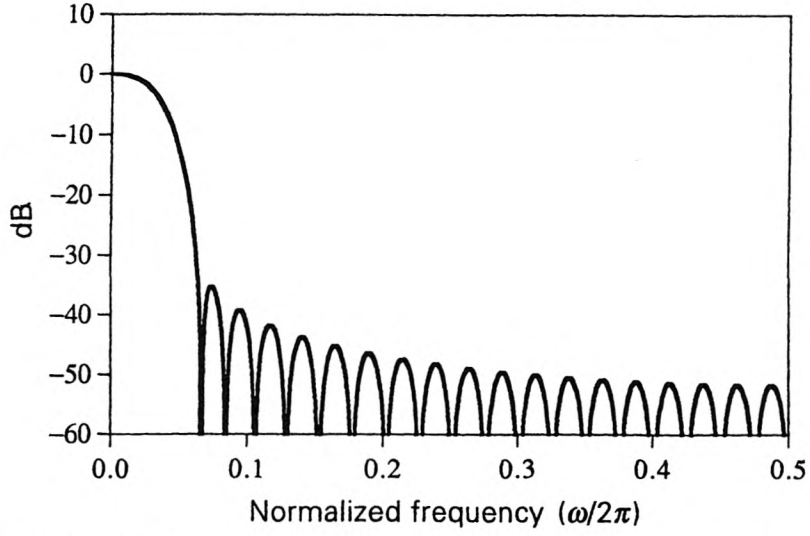

Figure 8.2-2 Design example 8.2.1. Pseudo QMF design. Magnitude response of the FIR linear phase prototype $P_0(z)$. Filter order $N = 39$.

Peak distortions $\mathbf{E_a}$ and $\mathbf{E_{pp}}$. Let us now look at various distortions. Recall that (5.4.7) represents the gain for the ℓth alias component $X(zW^\ell), \ell > 0$. Fig. 8.2-4 shows a plot of

$$\sqrt{\sum_{\ell=1}^{M-1} |A_\ell(e^{j\omega})|^2}, \tag{8.2.10}$$

which demonstrates that each of the terms $|A_\ell(e^{j\omega})|$ is very small for all ω. This shows that aliasing has been reduced satisfactorily. The quantity E_a, which is the maximum value of (8.2.10) over all ω, is the worst possible *peak aliasing distortion.*

Next, Fig. 8.2-5 shows a plot of $M|T(e^{j\omega})|$. This is very close to unity for all ω, verifying that amplitude distortion has been reduced satisfactorily. As argued earlier, $|T(e^{j\omega})|$ is seen to have period $2\pi/2M = \pi/8$. By design, $T(z)$ has linear phase, so we need not worry about phase distortion. The maximum peak to peak ripple of $M|T(e^{j\omega})|$, denoted E_{pp}, is usually taken to be a measure of worst possible amplitude distortion.

From (8.1.20) we see that $T(z)$ has order 78, i.e., $T(z) = \sum_{n=0}^{78} t(n)z^{-n}$. Because of the form (8.2.3), only a subset of the coefficients $t(n)$ are nonzero. The coefficients $Mt(n)$ are shown in Table 8.2.2, which also verifies the linear phase nature of $T(z)$. In fact, we see that $T(z)$ is nearly a delay.

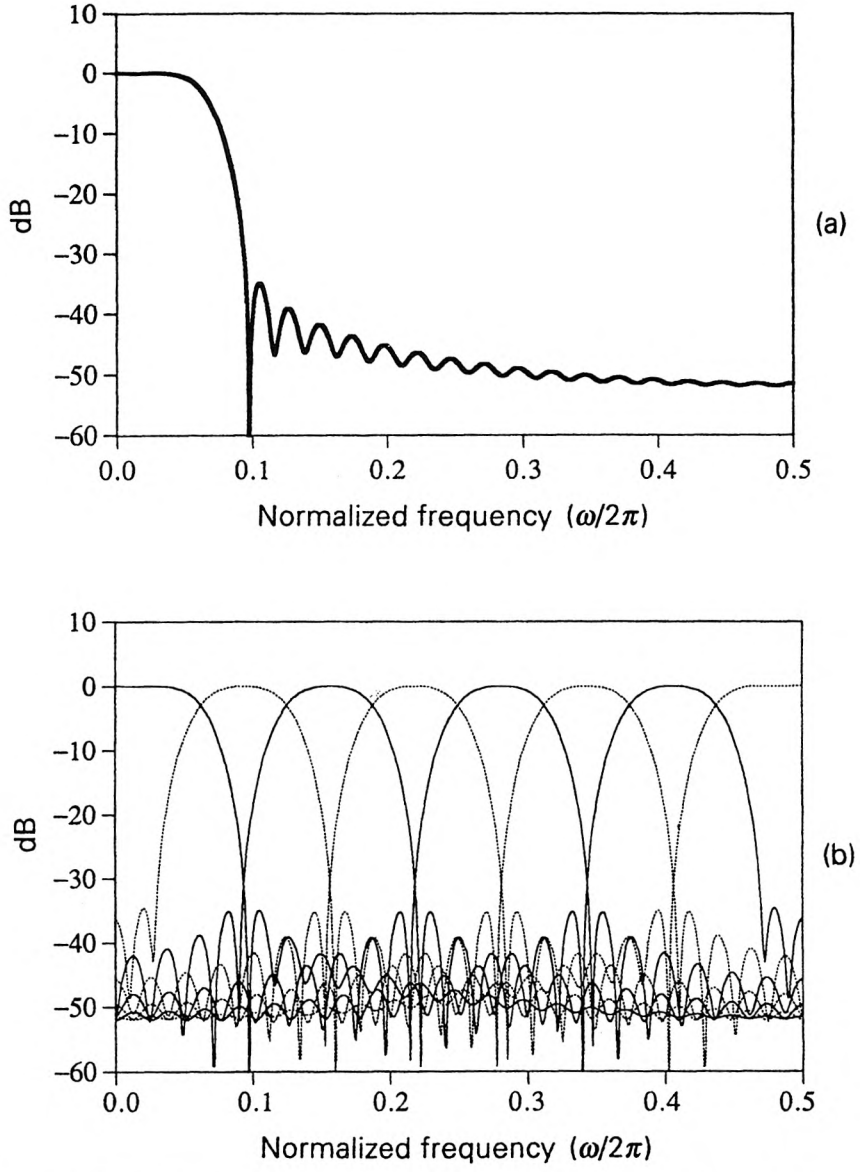

Figure 8.2-3 Design example 8.2.1. Pseudo QMF design. Magnitude responses of the analysis filters. (a) $H_0(z)$ only, and (b) all eight filters. Filter order $N = 39$; number of channels $M = 8$.

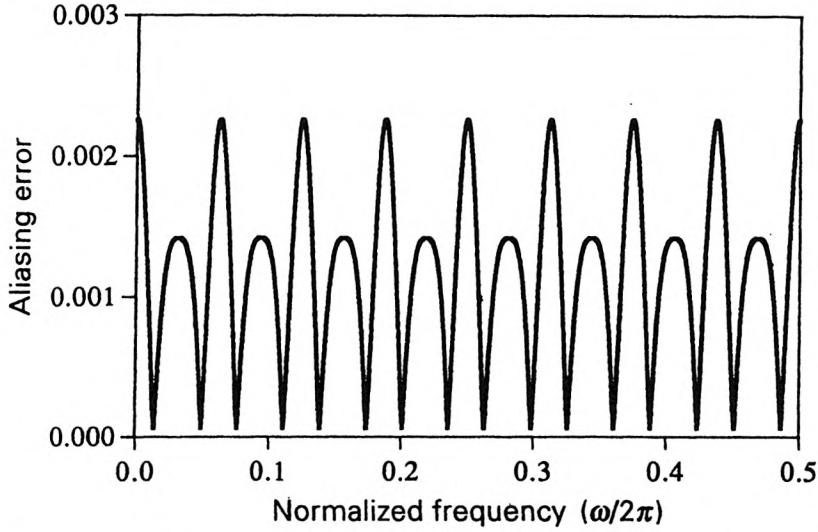

Figure 8.2-4 Design example 8.2.1. Plot of aliasing error in pseudo QMF design. The quantity (8.2.10) is shown above.

TABLE 8.2.2 Design example 8.2.1. Set of nonzero coefficients of $MT(z)$ where $T(z)$ is the distortion function for the pseudo QMF design.

n	$Mt(n)$
7	0.0022752
23	0.0008191
39	0.9988325
55	0.0008191
71	0.0022752

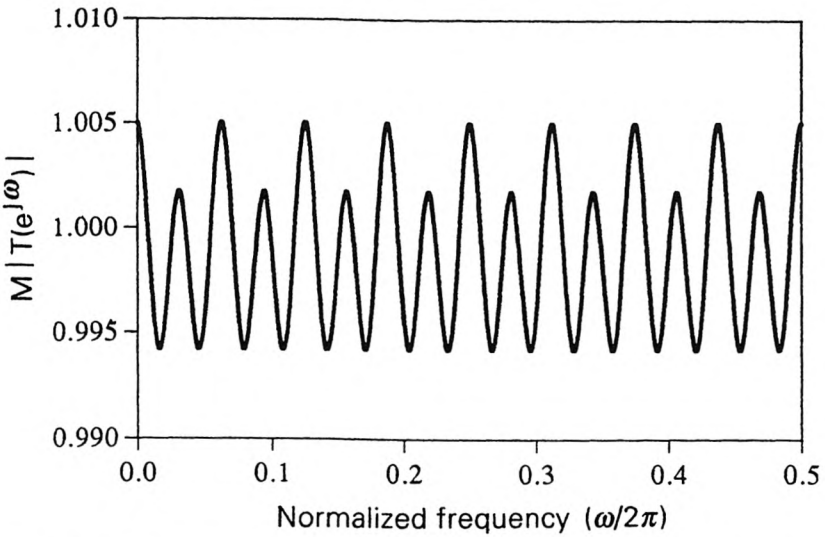

Figure 8.2-5 Design example 8.2.1. Plot of amplitude distortion function in pseudo QMF bank.

8.3 EFFICIENT POLYPHASE STRUCTURES

With the constants a_k, b_k and c_k constrained as summarized at the end of Sec. 8.1.3, we can rewrite the expression for the analysis filters as

$$H_k(z) = d_k Q_k(z) + d_k^* Q_{2M-1-k}(z) \tag{8.3.1}$$

with $0 \leq k \leq M-1$. Here

$$d_k = a_k c_k = e^{j\theta_k} W^{(k+0.5)N/2}, \quad 0 \leq k \leq M-1. \tag{8.3.2}$$

Since the coefficients of $Q_{2M-1-k}(z)$ are conjugates of those of $Q_k(z)$, $h_k(n)$ are real as intended. As the filters $Q_k(z)$ can be represented by the structure of Fig. 8.1-3, we can implement the M analysis filters as in Fig. 8.3-1(a). From this figure we can write

$$H_k(z) = \sum_{n=0}^{2M-1} t_{kn} z^{-n} G_n(-z^{2M}), \quad 0 \leq k \leq M-1, \tag{8.3.3}$$

where

$$t_{kn} = W^{-(k+0.5)(n-\frac{N}{2})} e^{j\theta_k} + W^{(k+0.5)(n-\frac{N}{2})} e^{-j\theta_k}. \tag{8.3.4}$$

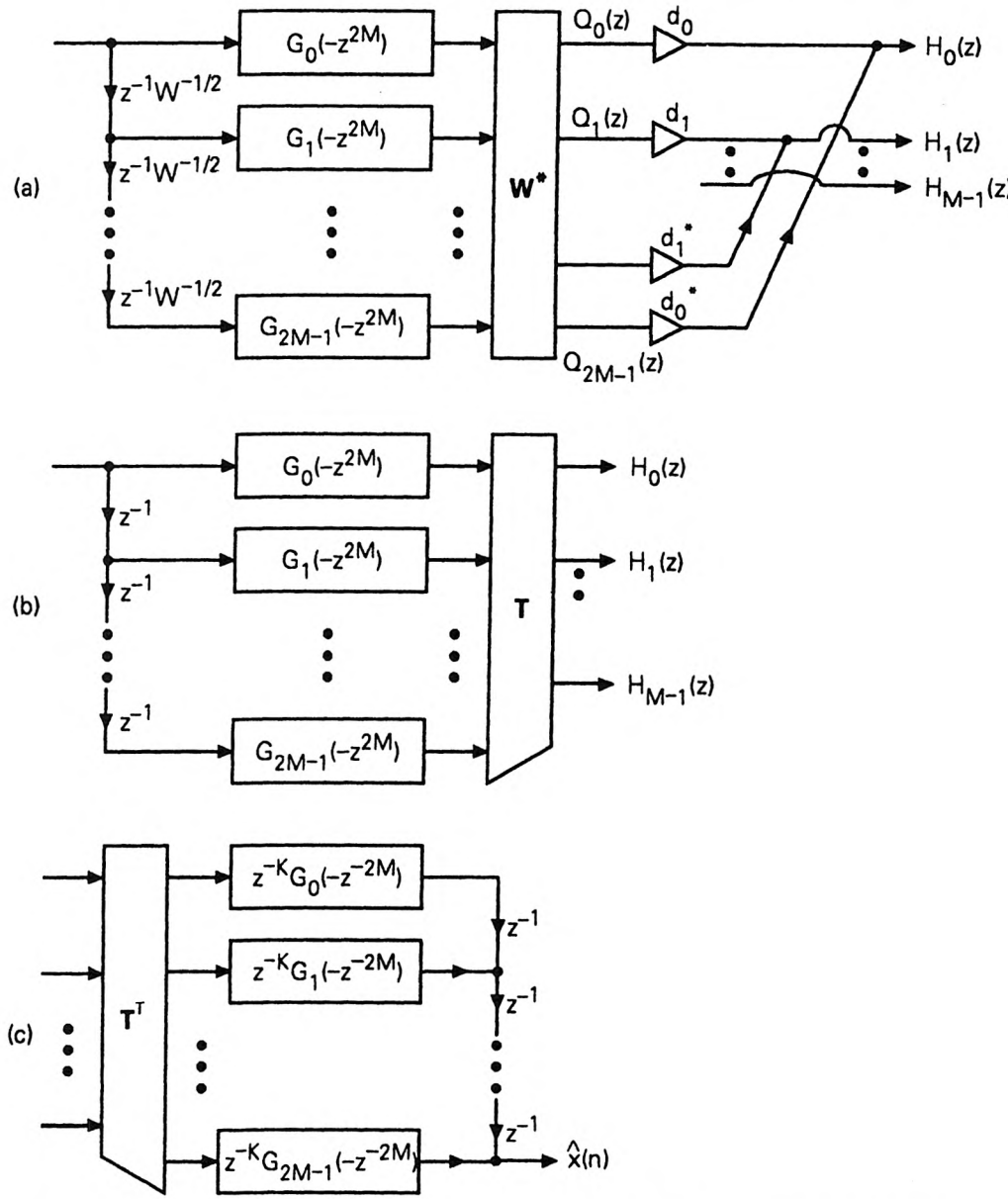

Figure 8.3-1 (a) Polyphase implementation of the M-channel cosine modulated analysis bank, (b) simplified drawing, where $\mathbf{T}$ is a real matrix, and (c) corresponding synthesis bank. Here $K = N - 2M + 1$.

The elements t_{kn} simplify to

$$t_{kn} = 2\cos\Big(\frac{\pi}{M}(k+0.5)(n-\frac{N}{2}) + \theta_k\Big), \tag{8.3.5}$$

where $\theta_k = (-1)^k\pi/4$. Equation (8.3.3) permits us to draw the analysis bank as in Fig. 8.3-1(b), where $\mathbf{T}$ is $M \times 2M$ with elements t_{kn}. Note that the coefficients t_{kn} are precisely the elements which modulate $p_0(n)$ in (8.1.37) to obtain $h_k(n)$. The M cosine modualted filters $H_k(z)$ are therefore obtained by implementing the polyphase components $G_n(-z^{2M})$ which come from the single prototype $P_0(z)$, and then using the cosine modulation matrix $\mathbf{T}$.

In terms of matrix notation, the analysis bank vector $\mathbf{h}(z)$ defined in (5.4.1) becomes

$$\mathbf{h}(z) = \mathbf{T}\mathbf{g}(z), \tag{8.3.6}$$

where

$$\mathbf{g}(z) \triangleq \begin{bmatrix} G_0(-z^{2M}) \\ z^{-1}G_1(-z^{2M}) \\ \vdots \\ z^{-(2M-1)}G_{2M-1}(-z^{2M}) \end{bmatrix}. \tag{8.3.7}$$

To obtain the structure for the synthesis bank we use the relation $F_k(z) = z^{-N}H_k(z^{-1})$, and write the synthesis filter vector $\mathbf{f}(z)$ in terms of the analysis filter vector $\mathbf{h}(z)$ as

$$\mathbf{f}^T(z) = z^{-N}\mathbf{h}^T(z^{-1}) = z^{-N}\mathbf{g}^T(z^{-1})\mathbf{T}^T. \tag{8.3.8}$$

This system can be implemented as shown in Fig. 8.3-1(c), where the quantity $K = N - 2M + 1$.

In practice, we have decimators following the analysis filters, and expanders preceding the synthesis filters (Fig. 5.4.1). These devices can be moved by employing the noble identities (Fig. 4.2.3) to obtain more efficient polyphase structures. Figure 8.3-2 shows this scheme for the analysis bank, where the filters $G_n(-z^2)$ operate at the lowest possible rate. Similar arrangement can be obtained for the synthesis bank.

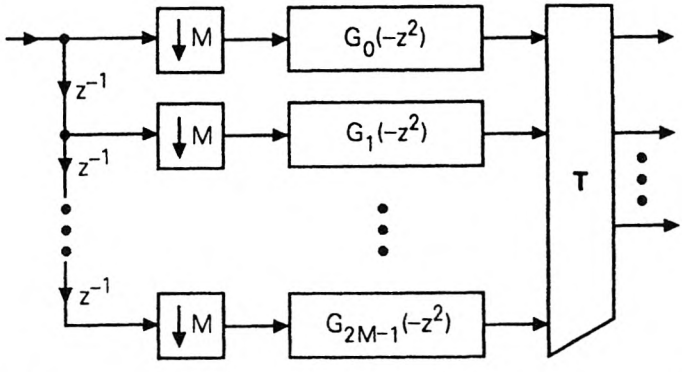

Figure 8.3-2 Improved polyphase implementation of the pseudo QMF analysis bank, with decimators moved "all the way to the left."

Implementation Using the Discrete Cosine Transform (DCT)

A special case of interest arises when the filter length $N+1$ is restricted to be $N+1 = 2mM$ for some integer m. In this case, the polyphase structure can be redrawn in such a way that the main computational load is represented by a $M \times M$ matrix called the discrete cosine transform (DCT). Moreover, this matrix can be implemented using fast transform techniques [Yip and Rao, 1987]. Details of this special case are developed in the next few sections, where we also show how to modify the results of the present section to achieve *perfect reconstruction* in cosine modulated QMF banks.

Computational Complexity of Pseudo QMF Systems

We can implement the analysis bank as in Fig. 8.3-1(b), where $G_k(z)$ are the $2M$ polyphase components of $P_0(z)$. The total number of multiplications and additions required for these components is nearly equal to the order N of the filter $P_0(z)$. So the complexity of the analysis bank is equal to about N multipliers and adders, plus the overhead required to implement the modulation matrix. The exact cost of this overhead depends on the value of M and the details of the fast DCT. Assuming this cost is negligible for simplicity, the complexity of the analysis bank is about N/M MPUs (and the same number of APUs). Recall from Sec. 6.7 that, for this *same filter order* N if $N >> M$, the perfect reconstruction system is only about two times more expensive.

8.4 DEEPER PROPERTIES OF COSINE MATRICES

The cosine modulation matrix $\mathbf{T}$ which appears in the pseudo QMF structure of Fig. 8.3-2 satisfies some very useful mathematical properties. These properties, while not obvious, are important in the design of *perfect reconstruction* cosine modulated filter banks, as we see in Sec. 8.5. The purpose of this section is to state and prove these properties.

8.4.1 The DCT and DST matrices

We first introduce the discrete cosine transform (DCT) matrix $\mathbf{C}$, and the the discrete sine transform (DST) matrix $\mathbf{S}$. These will play a crucial role in the theory as well as *fast* implementation of the cosine-modulated perfect reconstruction systems to be studied in Sec. 8.5.

The discrete cosine transform has been known since the early seventies [Ahmed, et al., 1974]. Four types of DCT and DST matrices have been documented in the literature [Yip and Rao, 1987]. Of these only Type 4 matrices are relevant to our discussion. These are $M \times M$ matrices with elements

$$c_{kn} = \sqrt{\frac{2}{M}} \cos \frac{\pi}{M}(k+0.5)(n+0.5), \quad s_{kn} = \sqrt{\frac{2}{M}} \sin \frac{\pi}{M}(k+0.5)(n+0.5). \tag{8.4.1}$$

We omit the adjective 'Type 4' in all further discussions. Evidently $\mathbf{C}$ and $\mathbf{S}$ are real. They satisfy the following properties.

1. Symmetry, that is, $\mathbf{C}^T = \mathbf{C}$, and $\mathbf{S}^T = \mathbf{S}$.
2. $\mathbf{C}$ and $\mathbf{S}$ are related as

$$\mathbf{C} = \mathbf{\Gamma S J}, \tag{8.4.2}$$

where

$$\mathbf{\Gamma} = \begin{bmatrix} 1 & 0 & 0 & \dots & 0 \\ 0 & -1 & 0 & \dots & 0 \\ \vdots & \vdots & \vdots & \ddots & \vdots \\ 0 & 0 & 0 & \dots & (-1)^{M-1} \end{bmatrix}, \tag{8.4.3}$$

and $\mathbf{J}$ is the reversal (or anti-diagonal) matrix defined in Appendix A (Sec. A.2). In words, if we renumber the nth column of $\mathbf{S}$ as the $(M-1-n)$th column (for each n), and insert a minus sign on all elements of every odd numbered row, the result is the $\mathbf{C}$ matrix. We can also rewrite (8.4.2) as $\mathbf{S} = \mathbf{\Gamma C J}$, since $\mathbf{\Gamma}^{-1} = \mathbf{\Gamma}$ and $\mathbf{J}^{-1} = \mathbf{J}$.

3. $\mathbf{C}$ and $\mathbf{S}$ are orthonormal, that is, $\mathbf{C}^T\mathbf{C} = \mathbf{S}^T\mathbf{S} = \mathbf{I}$. By combining with symmetry, we have $\mathbf{C}^2 = \mathbf{S}^2 = \mathbf{I}$ so that $\mathbf{C}^{-1} = \mathbf{C}$ and $\mathbf{S}^{-1} = \mathbf{S}$.

Proofs

The first property is obvious. A proof of the second property is requested in Problem 8.6. We will now prove the third property. It is sufficient to prove orthonormality of $\mathbf{C}$. Orthonormality of $\mathbf{S}$ then follows from $\mathbf{S} = \mathbf{\Gamma C J}$.

Orthonormality of C. Consider Fig. 8.4-1 which is a system with $2M$ inputs and M outputs. Here, $\mathbf{W}$ is the $2M \times 2M$ DFT matrix, $W = e^{-j2\pi/2M}$, and $\beta_n = W^{-(n+0.5)/2}$. This system has a $M \times 2M$ transfer matrix, which we denote as $\mathbf{V}$. This matrix has elements

$$\begin{aligned} V_{kn} &= \beta_k W^{-(k+0.5)n} + \beta_k^* W^{(k+0.5)n} \\ &= W^{-(k+0.5)(n+0.5)} + W^{(k+0.5)(n+0.5)} \\ &= 2\cos\frac{\pi}{M}(k+0.5)(n+0.5). \end{aligned}$$

So we can write

$$\mathbf{V} = \sqrt{2M}\,[\,\mathbf{C} \quad \times\,]. \tag{8.4.4}$$

In other words, except for the scale factor $\sqrt{2M}$, the first M columns of $\mathbf{V}$ are the same as those of $\mathbf{C}$. (The $\times$ denotes an $M \times M$ matrix whose details are not relevant here.) By using the structure of Fig. 8.4-1 one verifies that

$$\mathbf{C} = \frac{1}{\sqrt{2M}} \underbrace{[\,\mathbf{I} \quad -\mathbf{J}\,]}_{M \times 2M} \mathbf{\Lambda}_\beta \mathbf{U} \mathbf{\Lambda}_w, \tag{8.4.5}$$

where $\mathbf{\Lambda}_\beta$ and $\mathbf{\Lambda}_w$ are diagonal matrices of sizes $2M \times 2M$ and $M \times M$ respectively, with diagonal elements

$$[\mathbf{\Lambda}_\beta]_{kk} = \beta_k, \quad [\mathbf{\Lambda}_w]_{kk} = W^{-0.5k}, \tag{8.4.6}$$

and $\mathbf{U}$ is the left $2M \times M$ submatrix of $\mathbf{W}^*$. By using the fact that

$$\begin{bmatrix} \mathbf{I} \\ -\mathbf{J} \end{bmatrix} [\mathbf{I} \quad -\mathbf{J}] = \mathbf{I}_{2M} - \mathbf{J}_{2M},$$

we can verify

$$\mathbf{C}^T\mathbf{C} = \mathbf{C}^\dagger\mathbf{C} = \left(\mathbf{\Lambda}_w^\dagger\mathbf{U}^\dagger\mathbf{\Lambda}_\beta^\dagger\mathbf{\Lambda}_\beta\mathbf{U}\mathbf{\Lambda}_w - \mathbf{\Lambda}_w^\dagger\mathbf{U}^\dagger\mathbf{\Lambda}_\beta^\dagger\mathbf{J}_{2M}\mathbf{\Lambda}_\beta\mathbf{U}\mathbf{\Lambda}_w\right)/2M, \tag{8.4.7}$$

In Problem 8.7 we verify that the first term above is $2M\mathbf{I}$ and the second term is zero. This proves that $\mathbf{C}^T\mathbf{C} = \mathbf{I}$. ▽▽▽

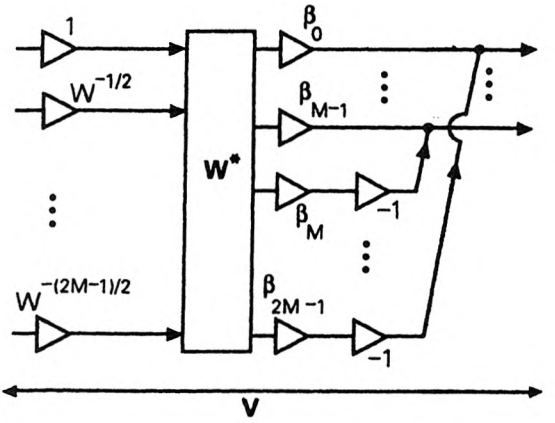

Figure 8.4-1 Pertaining to the proof that the DCT matrix is orthonormal.

8.4.2 Cosine Modulation Expressed Using DCT and DST

Consider the cosine modulation matrix $\mathbf{T}$ in the pseudo QMF structure of Fig. 8.3-2. We now show how this can be expressed in terms of the DCT and DST matrices. Recall that $\mathbf{T}$ is $M \times 2M$ with elements t_{kn} as in (8.3.5), where N is the order of the prototype filter.

We consider only the special case where the filter length $N+1$ and the number of channels M are related as

$$N + 1 = 2mM, \tag{8.4.8}$$

for some integer m. Let us partition $\mathbf{T}$ as

$$\mathbf{T} = [\mathbf{A}_0 \quad \mathbf{A}_1], \tag{8.4.9}$$

where $\mathbf{A}_0$ and $\mathbf{A}_1$ are $M \times M$. We will show that these matrices can be expressed in terms of the DCT and DST matrices as follows:

$$\mathbf{A}_0 = \sqrt{M}\mathbf{\Lambda}_c(\mathbf{C} - \mathbf{\Gamma}\mathbf{S}), \quad \mathbf{A}_1 = -\sqrt{M}\mathbf{\Lambda}_c(\mathbf{C} + \mathbf{\Gamma}\mathbf{S}) \quad (m \text{ even}), \tag{8.4.10}$$

$$\mathbf{A}_0 = \sqrt{M}\mathbf{\Lambda}_s\mathbf{\Gamma}(\mathbf{C} + \mathbf{\Gamma}\mathbf{S}), \quad \mathbf{A}_1 = \sqrt{M}\mathbf{\Lambda}_s\mathbf{\Gamma}(\mathbf{C} - \mathbf{\Gamma}\mathbf{S}) \quad (m \text{ odd}). \tag{8.4.11}$$

Here $\mathbf{\Lambda}_c$ and $\mathbf{\Lambda}_s$ are $M \times M$ diagonal matrices with diagonal elements

$$[\mathbf{\Lambda}_c]_{kk} = \cos\big(\pi(k + 0.5)m\big), \quad [\mathbf{\Lambda}_s]_{kk} = \sin\big(\pi(k + 0.5)m\big). \tag{8.4.12}$$

Notice that for fixed m, one of these two diagonal matrices is null, and the other has diagonal elements ± 1. Using the above expressions for $\mathbf{A}_0$ and $\mathbf{A}_1$ we will also show that they satisfy

$$\mathbf{A}_0^T\mathbf{A}_0 = 2M\big(\mathbf{I} - (-1)^m\mathbf{J}\big), \tag{8.4.13}$$

$$\mathbf{A}_1^T\mathbf{A}_1 = 2M\big(\mathbf{I} + (-1)^m\mathbf{J}\big), \tag{8.4.14}$$

$$\mathbf{A}_0^T\mathbf{A}_1 = \mathbf{0}. \tag{8.4.15}$$

Readers interested only in the consequences of these relations can skip the following proof, and proceed to Sec. 8.5.

Proof of the Relations (8.4.10)–(8.4.15)

For $N = 2mM - 1$, the elements t_{kn} in (8.3.5) become

$$t_{kn} = 2\Big(\widehat{c}_{kn}\cos\phi_k - \widehat{s}_{kn}\sin\phi_k\Big), \quad 0 \le k \le M-1, \; 0 \le n \le 2M-1, \tag{8.4.16}$$

where

$$\widehat{c}_{kn} = \cos\left(\frac{\pi}{M}(k + 0.5)(n + 0.5)\right), \quad \widehat{s}_{kn} = \sin\left(\frac{\pi}{M}(k + 0.5)(n + 0.5)\right), \tag{8.4.17}$$

and

$$\phi_k = -\pi(k + 0.5)m + (-1)^k\frac{\pi}{4}. \tag{8.4.18}$$

The elements of the $M \times M$ matrix $\mathbf{A}_0$ are therefore

$$[\mathbf{A}_0]_{kn} = 2\Big(\widehat{c}_{kn}\cos\phi_k - \widehat{s}_{kn}\sin\phi_k\Big), \quad 0 \le k, n \le M - 1. \tag{8.4.19}$$

The elements of $\mathbf{A}_1$ are found by replacing n with $n + M$ in (8.4.16), and simplifying. Thus

$$[\mathbf{A}_1]_{kn} = -2(-1)^k\Big(\widehat{s}_{kn}\cos\phi_k + \widehat{c}_{kn}\sin\phi_k\Big) \quad 0 \le k, n \le M - 1. \tag{8.4.20}$$

The quantities $\cos\phi_k$ and $\sin\phi_k$ can be simplified into

$$\begin{aligned}\cos\phi_k &= \frac{1}{\sqrt{2}}\Big(\cos\big(\pi(k+0.5)m\big) + (-1)^k \sin\big(\pi(k+0.5)m\big)\Big),\\ \sin\phi_k &= \frac{1}{\sqrt{2}}\Big(-\sin\big(\pi(k+0.5)m\big) + (-1)^k \cos\big(\pi(k+0.5)m\big)\Big).\end{aligned} \tag{8.4.21}$$

Using the diagonal matrices $\mathbf{\Lambda}_c$ and $\mathbf{\Lambda}_s$ we can then express

$$\begin{aligned}\mathbf{A}_0 &= \sqrt{M}\Big((\mathbf{\Lambda}_c + \mathbf{\Gamma}\mathbf{\Lambda}_s)\mathbf{C} - (-\mathbf{\Lambda}_s + \mathbf{\Gamma}\mathbf{\Lambda}_c)\mathbf{S}\Big),\\ \mathbf{A}_1 &= -\sqrt{M}\mathbf{\Gamma}\Big((\mathbf{\Lambda}_c + \mathbf{\Gamma}\mathbf{\Lambda}_s)\mathbf{S} + (-\mathbf{\Lambda}_s + \mathbf{\Gamma}\mathbf{\Lambda}_c)\mathbf{C}\Big).\end{aligned} \tag{8.4.22}$$

Depending on the value of m, this expression can be simplified further. If m is even then $\mathbf{\Lambda}_s = \mathbf{0}$ and $[\mathbf{\Lambda}_c]_{kk} = \pm 1$. If m is odd, then the opposite situation prevails. This leads to the simplified relations claimed in (8.4.10) and (8.4.11).

If m is even, we find from (8.4.10)

$$\mathbf{A}_0^T\mathbf{A}_0 = M(\mathbf{C}^2 + \mathbf{S}^2 - \mathbf{C}\mathbf{\Gamma}\mathbf{S} - \mathbf{S}\mathbf{\Gamma}\mathbf{C}), \tag{8.4.23}$$

$$\mathbf{A}_1^T\mathbf{A}_1 = M(\mathbf{C}^2 + \mathbf{S}^2 + \mathbf{C}\mathbf{\Gamma}\mathbf{S} + \mathbf{S}\mathbf{\Gamma}\mathbf{C}), \tag{8.4.24}$$

$$\mathbf{A}_0^T\mathbf{A}_1 = -M(\mathbf{C}^2 - \mathbf{S}^2 + \mathbf{C}\mathbf{\Gamma}\mathbf{S} - \mathbf{S}\mathbf{\Gamma}\mathbf{C}), \tag{8.4.25}$$

The three properties of $\mathbf{C}$ and $\mathbf{S}$ listed at the beginning of Sec. 8.4.1 imply, in particular, $\mathbf{C}^2 = \mathbf{S}^2 = \mathbf{I}$, and $\mathbf{C}\mathbf{\Gamma}\mathbf{S} = \mathbf{S}\mathbf{\Gamma}\mathbf{C} = \mathbf{J}$. As a result the above relations reduce to (8.4.13)–(8.4.15) indeed. For odd m the proof can be carried out similarly. ▽▽▽

8.5 COSINE MODULATED PERFECT RECONSTRUCTION SYSTEMS

By using the results of the previous sections, it is now very easy to obtain a maximally decimated FIR perfect reconstruction system in which the analysis filters are related by cosine modulation [as in (8.1.37)], and the synthesis filters are as in (8.1.19a). This observation was made independently by Malvar [1990b], Ramstad [1991] and Koilpillai and Vaidyanathan, [1991 and 1992]. Among all FIR perfect reconstruction systems known today for arbitrary filter lengths, this system is perhaps the simplest (both in terms of design and implementation complexities). It inherits all the simplicity and elegance of the cosine modulated pseudo QMF system and yet offers perfect reconstruction property. We now proceed to derive this. Historically, a special case of this result for $N = 2M - 1$ was first reported [Princen and Bradley, 1986], [Malvar and Staelin, 1989], and is related to the concept of lapped orthogonal transforms (LOT, Sec. 6.6). The result of this section

can be considered to be a generalization of the LOT, and is presented in Malvar [1990b] in that light. Our presentation here is based on Koilpillai and Vaidyanathan [1991a, 1992].

Expression for the Polyphase Matrix E(z)

For the cosine modulated system the analysis bank has the structure shown in Fig. 8.3-1(b), where $G_k(z)$ are the $2M$ polyphase components of the prototype $P_0(z)$ (see Fig. 8.1-1). Thus,

$$\begin{aligned} \mathbf{h}(z) &= \mathbf{T} \begin{bmatrix} \mathbf{g}_0(z^{2M}) & \mathbf{0} \\ \mathbf{0} & \mathbf{g}_1(z^{2M}) \end{bmatrix} \begin{bmatrix} \mathbf{e}(z) \\ z^{-M}\mathbf{e}(z) \end{bmatrix}, \\ &= \mathbf{T} \begin{bmatrix} \mathbf{g}_0(z^{2M}) \\ z^{-M}\mathbf{g}_1(z^{2M}) \end{bmatrix} \mathbf{e}(z) \end{aligned} \tag{8.5.1}$$

where $\mathbf{e}(z)$ is the delay chain vector [eqn. (5.4.1)] and $\mathbf{g}_i(z)$ are diagonal matrices with

$$[\mathbf{g}_0(z)]_{kk} = G_k(-z), \quad [\mathbf{g}_1(z)]_{kk} = G_{M+k}(-z). \tag{8.5.2}$$

Comparing with $\mathbf{h}(z) = \mathbf{E}(z^M)\mathbf{e}(z)$, we identify the polyphase matrix $\mathbf{E}(z)$ of the analysis bank as

$$\mathbf{E}(z) = \mathbf{T} \begin{bmatrix} \mathbf{g}_0(z^2) \\ z^{-1}\mathbf{g}_1(z^2) \end{bmatrix}. \tag{8.5.3}$$

Using the partition $\mathbf{T} = [\,\mathbf{A}_0 \quad \mathbf{A}_1\,]$ as before, we have

$$\mathbf{E}(z) = [\,\mathbf{A}_0 \quad \mathbf{A}_1\,] \begin{bmatrix} \mathbf{g}_0(z^2) \\ z^{-1}\mathbf{g}_1(z^2) \end{bmatrix}. \tag{8.5.4}$$

8.5.1 Forcing E(z) to be Paraunitary when N + 1 = 2mM

From Chapter 6 we know that we can achieve perfect reconstruction by constraining $\mathbf{E}(z)$ to be paraunitary (i.e., $\widetilde{\mathbf{E}}(z)\mathbf{E}(z) = d\mathbf{I}$) and taking the synthesis filter coeffcients to be the time reversed conjugates as in (6.2.6). Recall that the paraunitary property is the same as losslessness, since we are discussing only causal FIR systems. The main result is summarized as follows:

♠**Theorem 8.5.1.** Let the prototype $P_0(z)$ be a real-coefficient FIR filter with length $N+1 = 2mM$ for some integer m. Assume $p_0(n) = p_0(N-n)$ (linear phase constraint). Let $G_k(z)$, $0 \le k \le 2M-1$, be the $2M$ polyphase components of $P_0(z)$. Suppose the M analysis filters $H_k(z)$ are generated by cosine modulation as in (8.1.37) with $\theta_k = (-1)^k\pi/4$. Then

the $M \times M$ polyphase component matrix $\mathbf{E}(z)$ is paraunitary if, and only if, $G_k(z)$ satisfy the pairwise power complementary conditions

$$\widetilde{G}_k(z)G_k(z) + \widetilde{G}_{M+k}(z)G_{M+k}(z) = \alpha, \quad 0 \le k \le M-1, \tag{8.5.5}$$

for some $\alpha > 0$. ◊

Proof. From (8.5.4) we have

$$\begin{aligned}\widetilde{\mathbf{E}}(z)\mathbf{E}(z) =& \widetilde{\mathbf{g}}_0(z^2)\mathbf{A}_0^T\mathbf{A}_0\mathbf{g}_0(z^2) + \widetilde{\mathbf{g}}_1(z^2)\mathbf{A}_1^T\mathbf{A}_1\mathbf{g}_1(z^2) \\ &+ z\widetilde{\mathbf{g}}_1(z^2)\mathbf{A}_1^T\mathbf{A}_0\mathbf{g}_0(z^2) + z^{-1}\widetilde{\mathbf{g}}_0(z^2)\mathbf{A}_0^T\mathbf{A}_1\mathbf{g}_1(z^2).\end{aligned} \tag{8.5.6}$$

Since $\mathbf{A}_0$ and $\mathbf{A}_1$ satisfy (8.4.13)–(8.4.15), this becomes

$$\begin{aligned}\widetilde{\mathbf{E}}(z)\mathbf{E}(z) =& 2M\Big(\widetilde{\mathbf{g}}_0(z^2)\mathbf{g}_0(z^2) + \widetilde{\mathbf{g}}_1(z^2)\mathbf{g}_1(z^2)\Big) \\ &- 2M(-1)^m\Big(\widetilde{\mathbf{g}}_0(z^2)\mathbf{J}\mathbf{g}_0(z^2) - \widetilde{\mathbf{g}}_1(z^2)\mathbf{J}\mathbf{g}_1(z^2)\Big).\end{aligned} \tag{8.5.7}$$

Since $N+1 = 2mM$, each polyphase component $G_k(z)$ has length m, that is, order $m-1$. The relation $p_0(n) = p_0(N-n)$ imposes the following constraint on these polyphase components (Problem 8.8):

$$G_k(z) = z^{-(m-1)}\widetilde{G}_{2M-1-k}(z) \quad \text{(linear phase constraint).} \tag{8.5.8a}$$

In other words the diagonal matrices $\mathbf{g}_0(z)$ and $\mathbf{g}_1(z)$ are related as

$$\mathbf{g}_1(z) = z^{-(m-1)}(-1)^{m-1}\mathbf{J}\widetilde{\mathbf{g}}_0(z)\mathbf{J} \quad \text{(linear phase constraint).} \tag{8.5.8b}$$

(Recall from Appendix A (Sec. A.2) that **JDJ** has the effect of reversing the order of the diagonal entries of a diagonal matrix **D**.) If this relation is used in (8.5.7), the second term vanishes, and

$$\widetilde{\mathbf{E}}(z)\mathbf{E}(z) = 2M\Big(\widetilde{\mathbf{g}}_0(z^2)\mathbf{g}_0(z^2) + \widetilde{\mathbf{g}}_1(z^2)\mathbf{g}_1(z^2)\Big). \tag{8.5.9}$$

It is now clear that $\mathbf{E}(z)$ is paraunitary if, and only if,

$$\widetilde{\mathbf{g}}_0(z)\mathbf{g}_0(z) + \widetilde{\mathbf{g}}_1(z)\mathbf{g}_1(z) = \alpha\mathbf{I}, \quad \alpha > 0. \tag{8.5.10}$$

This condition is equivalent to saying that the polyphase components $G_k(z)$ and $G_{M+k}(z)$ are power complementary, that is, that (8.5.5) holds. ▽▽▽

Remark. The cosine modulated pseudo QMF system developed in Sec. 8.1 and 8.2 satisfies the relation (8.1.19a). Furthermore if the filters are

well-designed as described in Sec. 8.2, the system is almost like a perfect reconstruction system (as demonstrated by Design example 8.2.1). This suggests, in view of Theorem 6.2.1, that $\mathbf{E}(z)$ is "almost paraunitary". This leads us to expect that $\widetilde{\mathbf{E}}(z)\mathbf{E}(z)$ is "almost a diagonal matrix," and the diagonal elements are "almost constant." This, indeed, has been verified with the help of several design examples. This also shows that, if we force the matrix $\mathbf{E}(z)$ to be paraunitary *apriori*, that is, before optimizing the filter coefficients, then the resulting filters are almost the same as the pseudo QMF filters, except that they satisfy the perfect reconstruction property "perfectly"!

8.5.2 The Design Procedure

We know that all the analysis filter responses are controlled by the prototype response $|P_0(e^{j\omega})|$. As in Sec. 8.2.2 we have to optimize the coefficients of $P_0(z)$ to minimize an objective function. For pseudo QMF design we minimized a linear combination of ϕ_1 and ϕ_2 [defined in (8.2.7) and (8.2.8)]. But in the present case, it is sufficient to minimize only the stopband energy ϕ_2. The quantity ϕ_1 which represents the degree of nonflatness of $|T(e^{j\omega})|$ is automatically zero, because of the perfect reconstruction property guaranteed by paraunitariness of $\mathbf{E}(z)$.

Instead of minimizing the stopband energy ϕ_2, it is also possible to minimize the maximum magnitude of $|P_0(e^{j\omega})|$ in its stopband region. Either of these minimizations can be done using standard optimization routines [Press, et al., 1989], [IMSL, 1987].

Imposing Paraunitary Constraint Using Two-Channel Lattice

During optimization it is however necessary to impose the paraunitary constraint on $\mathbf{E}(z)$, which we have shown to be equivalent to the power complementary constraint (8.5.5). Now the power complementary property is equivalent to the condition that the FIR vector $\begin{bmatrix} G_k(z) \\ G_{M+k}(z) \end{bmatrix}$ be paraunitary. In a manner similar to Sec. 6.4, this paraunitary vector can be implemented with the cascaded lattice structure of Fig. 8.5-1. (This will be proved in Sec. 14.3.2). Conversely, the transfer functions $G_k(z)$ and $G_{M+k}(z)$ in this structure remain power complementary [i.e., satisfies (8.5.5) with $\alpha = 1$] regardless of the values of the angular parameters $\theta_{k,\ell}$. This follows because the matrices $\mathbf{R}_{k,\ell}$ are unitary; see Sec. 6.1.2.

The cosine modulated analysis bank, shown earlier in Fig. 8.3-2., now takes the appearance shown in Fig. 8.5-2. We now optimize the angles $\theta_{k,\ell}$ so as to minimize ϕ_2. During optimization, each lattice section remains paraunitary regardless of the values of $\theta_{k,\ell}$ so that the pair $\big(G_k(z), G_{M+k}(z)\big)$ remains power complementary (i.e., satisfies (8.5.5) with $\alpha = 1$). Thus, at the end of optimization, the matrix $\mathbf{E}(z)$ remains paraunitary, guaranteeing perfect reconstruction.

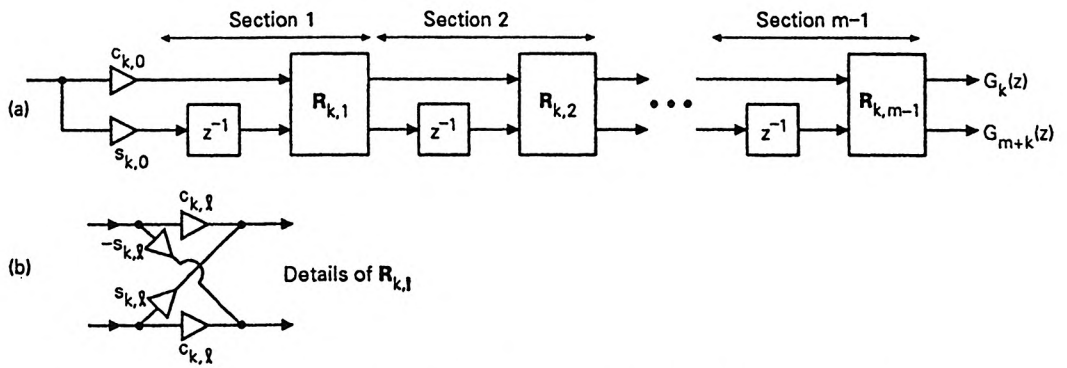

Figure 8.5-1 (a) Representation of the power complementary pair of functions $[G_k(z), G_{M+k}(z)]$ using a lossless lattice. (b) Details of $\mathbf{R}_{k,\ell}$. Here $c_{k,\ell} = \cos\theta_{k,\ell}$ and $s_{k,\ell} = \sin\theta_{k,\ell}$.

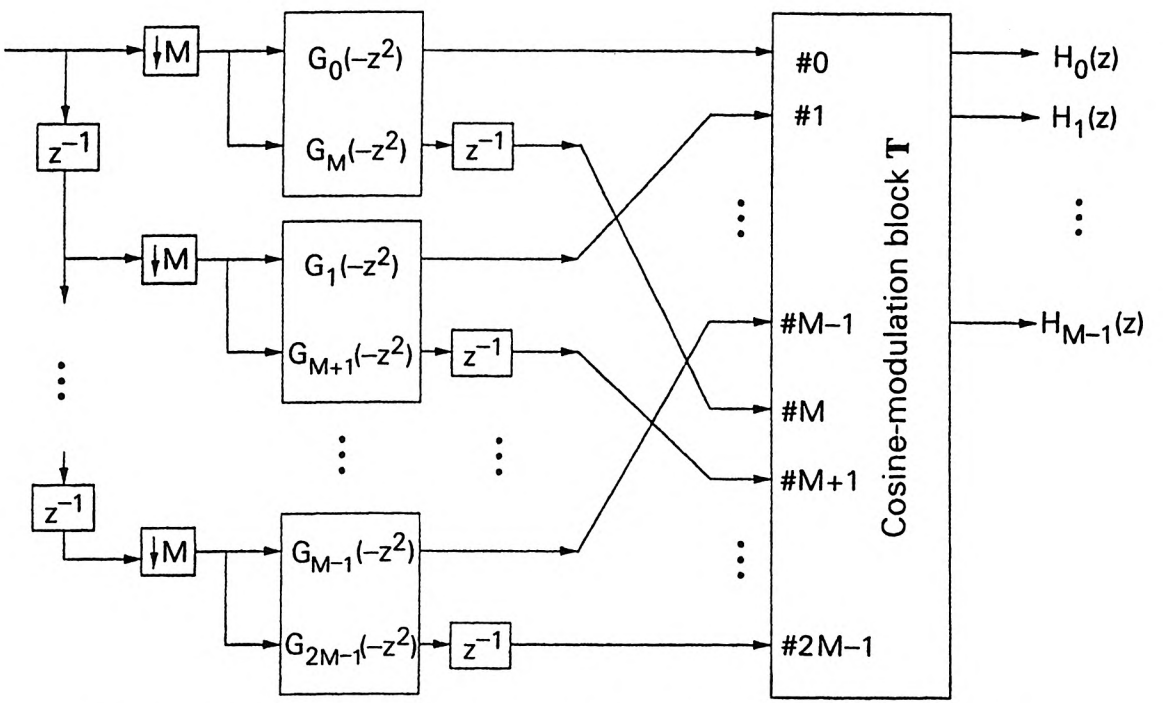

Figure 8.5-2 Implementation of cosine modulated PR analysis filter bank. Each polyphase component pair $[G_k(-z^2), G_{M+k}(-z^2)]$ is implemented by a two-channel lossless lattice.

Number of parameters to be optimized. In view of the linear-phase relation (8.5.8a), only $M/2$ lattice sections [$(M-1)/2$ for odd M; see below] need to be optimized. For example, let $M = 17$. Since $2M = 34$, there are 34 polyphase components $G_k(z)$. The pair $[G_0(z), G_{17}(z)]$ is generated using one lattice structure, the pair $[G_1(z), G_{18}(z)]$ using another lattice structure, and so on. Thus the first eight lattice structures generate the sixteen polyphase components

$$G_0(z), \ldots G_7(z), \quad \text{and} \quad G_{17}(z), \ldots G_{24}(z). \tag{8.5.11}$$

From these we can find the sixteen polyphase components

$$G_{33}(z), \ldots G_{26}(z), \quad \text{and} \quad G_{16}(z), \ldots G_9(z), \tag{8.5.12}$$

by use of the linear phase constraint (8.5.8a). There are two more components $G_8(z)$ and $G_{25}(z)$ to be determined. But the linear phase constraint implies

$$G_8(z) = z^{-(m-1)} \widetilde{G}_{25}(z), \tag{8.5.13}$$

so that (8.5.5) reduces to

$$\widetilde{G}_8(z) G_8(z) + \widetilde{G}_8(z) G_8(z) = 1. \tag{8.5.14}$$

Thus we have to choose $G_8(z) = \sqrt{0.5\alpha} z^{-K}$ and $G_{25}(z) = \sqrt{0.5\alpha} z^{-(m-1-K)}$.

For odd M, we can generalize this discussion and show (Problem 8.9) that

$$G_{\frac{M-1}{2}}(z) = \sqrt{0.5\alpha} z^{-K}, \quad \text{and} \quad G_{\frac{3M-1}{2}}(z) = \sqrt{0.5\alpha} z^{-(m-1-K)}.$$

Using the fact that $P_0(z)$ is a lowpass filter with cutoff $\pi/2M$ [Fig. 8.1-2(a)], it can be shown (Problem 8.9) that the only acceptable choice of K is given by

$$K = \begin{cases} \dfrac{m-1}{2} & \text{for odd } m, \\ \dfrac{m}{2} & \text{for even } m. \end{cases} \tag{8.5.15}$$

Thus, K is completely determined. Moreover α does not affect frequency responses except for a scale factor. Thus, the only parameters to be optimized are the parameters $\theta_{k,\ell}$ of the eight lattice structures.

More generally, the number of parameters to be optimized is nearly equal to $mM/2 \approx N/4$, which is half the number required for the pseudo QMF approach! This technique for design of perfect reconstruction systems is, therefore, simpler than the pseudo QMF design, and dramatically simpler than the (more general) perfect reconstruction design described in Sec. 6.5.

Hierarchial property. If we wish to increase the prototype length, we have to do it in integer multiples of $2M$ (because of the constraint $N + 1 =$

$2mM$). This can be done as shown in Fig. 8.5-3, where one new section is added to each lattice structure. This hierarchial approach can be used in the design process, to recursively intialize the parameters to be optimized. Thus we optimize the angles $\theta_{k,\ell}$ for small m, and then use these as initial values with m replaced by $m+1$. (The newly introduced parameters $\theta_{k,m}$ have to be initialized rather arbitrarily.) ‡

Obtaining the analysis and synthesis filters. Once the prototype coefficients $p_0(n)$ are obtained as above, the M analysis filters are found from (8.1.37). The synthesis filters are then obtained as $f_k(n) = h_k(N-n)$. In general these do not have linear phase, even though $P_0(z)$ does.

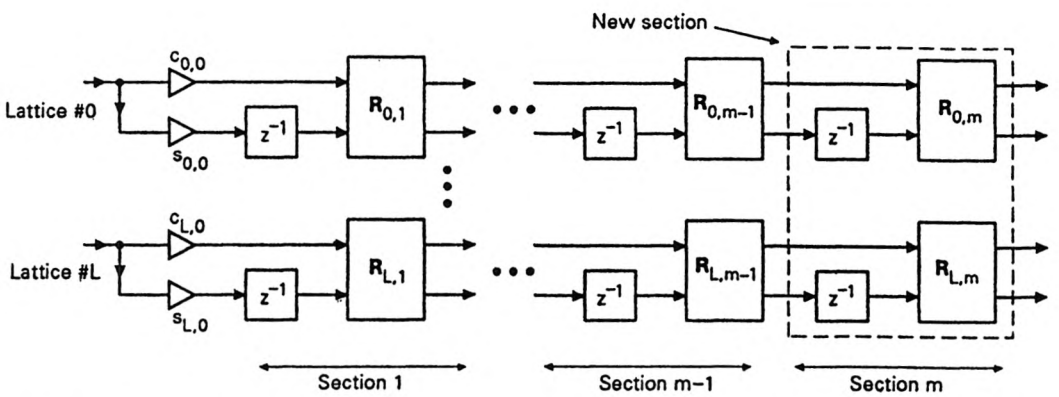

Figure 8.5-3 Explaining the hierarchial property of lattice-based design. $L+1$ is the number of lattice sections to be optimized.

Design Example 8.5.1: Cosine Modulated PR Systems

Let the number of channels be $M = 17$. For this choice of M we showed above that only eight lattice structures have to be optimized. Suppose the prototype filter $P_0(z)$ has order $N = 101$, so that $m = 3$. The kth lattice structure now has three angular parameters

$$\theta_{k,\ell}, \quad 0 \le k \le 7, 0 \le \ell \le 2.$$

These 24 parameters are optimized to minimize the peak stopband error of $P_0(z)$. Figure 8.5-4 shows the magnitude responses of $P_0(z)$ and all the

‡ See Koilpillai and Vaidyanathan [1992], for further details about initialization. A computer program, along with documentation, is available upon request.

17 analysis filters. Each analysis filter offers a stopband attenuation of about 40 dB. The impulse response $p_0(n)$ of the optimized prototype $P_0(z)$ is tabulated in Koilpillai and Vaidyanathan [1992].

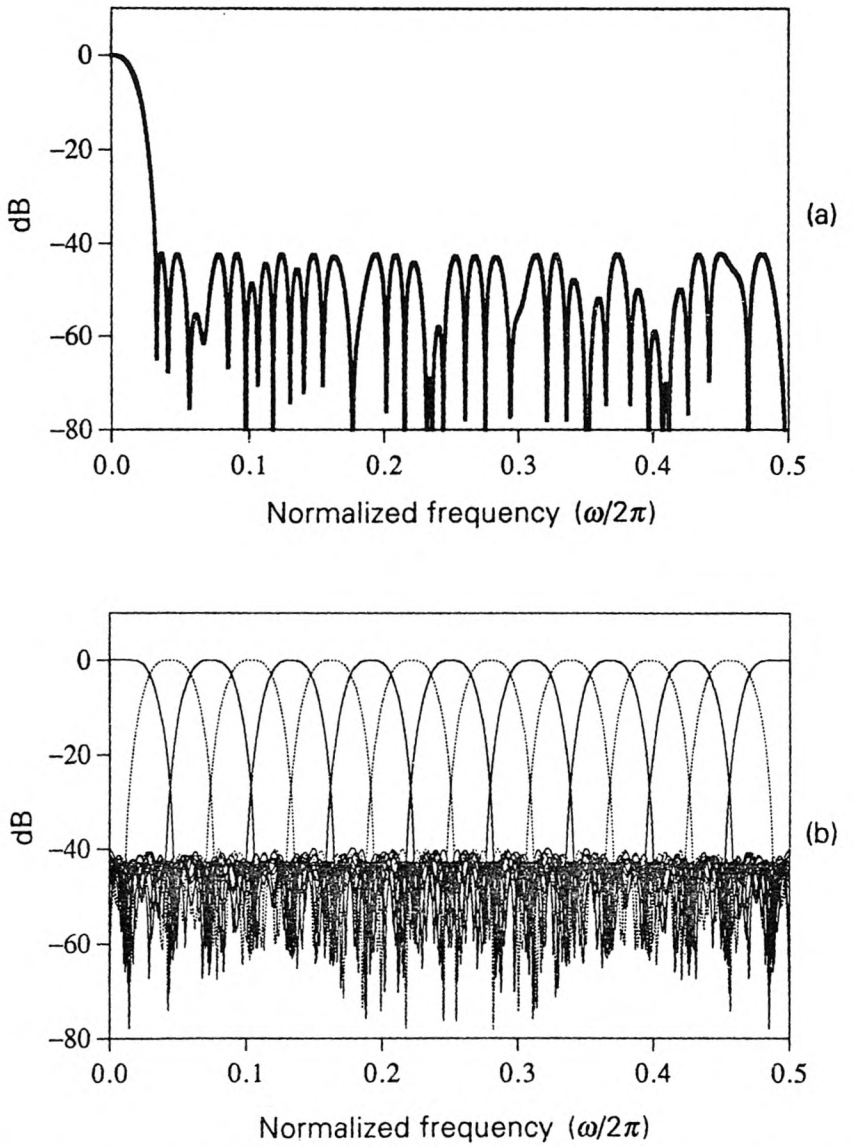

Figure 8.5-4 Design Example 8.5-1. Magnitude responses for the 17-channel cosine modulated perfect reconstruction system. (a) Prototype of order $N = 101$ and (b) the seventeen analysis filters. (© Adopted from 1992 IEEE.)

In this example the number of parameters to be optimized is equal to 24. For the same filter length and number of channels, the pseudo QMF system

(Sec. 8.2) has 51 parameters to be optimized, whereas the more general perfect reconstruction system (Sec. 6.5) has as many as 216 parameters! The method described in this section therefore has the fewest parameters, resulting in much faster design time. A more thorough comparison is given in the next section.

8.5.3 Complexity Comparison

We will now compare three types of M-channel maximally decimated filter banks, in terms of design complexity as well as implementation complexity. Recall that the filter coefficients are real. The quantity N denotes the order of the analysis filters, and M is the number of channels. The three types are:

Type 1. The general perfect reconstruction system with paraunitary $\mathbf{E}(z)$ described in Sec. 6.5, where $\mathbf{E}(z)$ was represented as a cascade of paraunitary building blocks of the form (6.5.1).

Type 2. The cosine modulated pseudo QMF (approximate reconstruction) system of Sec. 8.2.

Type 3. The cosine modulated perfect reconstruction (PR) system derived in this section.

Design Complexity

The number of parameters to be optimized during the design of the analysis filters depends on N, M, and the type of filter bank. In Table 8.5.1 we have listed these, for the three types of filter banks. Table 8.5.2 shows this number for various choices of M and N. We see that for fixed N and M, the cosine modulated PR system has significantly fewer parameters to be optimized than either of the other methods.

Next, in Table 8.5.3 we compare the two cosine modulated systems for the specific case where $N = 101$ and $M = 17$. To describe this table, first recall that the pseudo QMF system suffers from reconstruction errors, that is, residual aliasing and amplitude distortions. In Sec. 8.2.2 we defined quantitative measures for the aliasing error E_a and the peak-to-peak amplitude distortion E_{pp}. By varying the parameter α in the composite objective function (8.2.9), we can obtain a tradeoff between A_s and these reconstruction errors. In Table 8.5.3 we have shown a number of such tradeoffs. (The error $\approx 10^{-15}$ in the PR case is due to machine precision.) For the same N and M, the table also shows the attentuation A_s obtainable for the perfect reconstruction system. It is clear that, when we pass from the cosine modulated pseudo QMF system to the perfect reconstruction system, we pay a price in terms of the stopband attenuation A_s. This price however is not severe; it is less than 5 dB in most practical examples.

TABLE 8.5.1 The number of real valued parameters to be optimized during the design phase, for the three types of FIR M-channel maximally decimated QMF banks.

General FIR paraunitary perfect reconstruction system (section 6.5) (Type 1)	Cosine modulated pseudo QMF (Type 2)	Cosine modulated perfect reconstruction (Type 3)
$(M-1)\left(\frac{N+1-M}{M}+\frac{M}{2}\right)$	$\left(\frac{N+1}{2}\right)$	$\left(\frac{N+1}{2}\right)\left(\frac{M-1}{2M}\right), M$ odd

$N+1$ = filter length, M = number of channels

TABLE 8.5.2 Number of real valued parameters to be optimized for three types of FIR QMF banks.

M	N+1	Number of parameters to be optimized for		
		General FIR paraunitary perfect reconstruction (Type 1)	Cosine modulated pseudo QMF (Type 2)	Cosine modulated perfect reconstruction (Type 3)
3	48 60	33 41	24 30	8 10
5	40 60	38 54	20 30	8 12
7	42 84	51 87	21 42	9 18
16	64 96	165 195	32 48	15 23
17	68 102	184 216	34 51	16 24

$N+1$ = Analysis filter length, M = Number of channels

Implementation Complexity

In Sec. 6.7 we summarized the cost of the Type 1 filter bank in terms of the number of multiplications and additions per unit time (MPUs and APUs). Both Type 2 and Type 3 systems are cosine modulated systems with polyphase implementation as in Fig. 8.3-2. If these are implemented

like this, the analysis bank requires nearly $(N+1)/M$ MPUs and N/M APUs in both cases, plus the cost of implementing the modulation matrix. This additional cost is independent of the filter order N, and depends only on M. Table 8.5.4 is a summary of the implementation costs. Once again, the cosine modulated pseudo QMF and PR systems have significantly lower complexity than the Type 1 perfect reconstruction system.

TABLE 8.5.3 Comparison of the two cosine modulated systems (pseudo QMF versus perfect reconstruction). $N = 101$ and $M = 17$.

	Prototype		Reconstruction Error (E_{pp})	Aliasing Error (E_a)
	A_S (dB)	ω_S		
Pseudo-QMF bank	40.65	0.0590π	6.790 e−03	3.794 e−04
	38.68	0.0585π	2.139 e−04	3.193 e−04
	38.42	0.0581π	8.749 e−05	8.113 e−04
Cosine-modulated PR bank	35.72	0.0586π	8.216 e−15	1.041 e−15

TABLE 8.5.4 Computational complexity of the analysis bank for three types of FIR M-channel maximally decimated QMF banks. For cosine modulated system, cost of modulation must be added to the above numbers.

Complexity	General FIR paraunitary perfect reconstruction system (section 6.5) (Paraunitary cascade implementation) (Type 1)	Cosine modulated pseudo QMF (Type 2)	Cosine modulated perfect reconstruction system (Type 3)
MPU	$\frac{2N}{M} + M$ $\cong \frac{2N}{M} (N \gg M)$	$\frac{N+1}{M}$	$\frac{N+1}{M}$
APU	$\frac{2N}{M} + \frac{(M-1)^2}{M}$ $\cong \frac{2N}{M} (N \gg M)$	$\frac{N}{M}$	$\frac{N}{M}$

$N + 1$ = filter length, M = number of channels

Implementation using the lattice. The cosine modulated PR system can be implemented directly using the lattice structures which generate the pairs of polyphase components (Fig. 8.5-1). The schematic for this is shown in Fig. 8.5-2. From Chapter 6 we know that the two-channel lattice structure can be redrawn with two-multiplier sections (Fig. 6.4-2), by extracting some scale factors. If this is done, the complexity of the analysis bank (i.e., the number of MPUs and APUs) remains nearly the same as for the direct polyphase implementation of Fig. 8.3-2.

8.5.4 Implementing Cosine Modulation with DCT and DST

In Sec. 8.4 we established a relation between the cosine modulation matrix $\mathbf{T} = [\mathbf{A}_0 \quad \mathbf{A}_1]$ and the DCT and DST matrices. These relations are given in (8.4.10), (8.4.11), and hold when $N + 1 = 2mM$. Based on this we can redraw the analysis bank entirely in terms of the DCT matrix $\mathbf{C}$. This holds for both types of cosine modulated systems, that is, Type 2 (pseudo QMF) and Type 3 (perfect reconstruction).

Case When m is Even

The details depend on whether m is even or odd. We assume that m is even. (We leave it to the reader to work out the odd m case.) Since $\mathbf{S} = \boldsymbol{\Gamma}\mathbf{C}\mathbf{J}$ we can rewrite these entirely in terms of $\mathbf{C}$ to obtain

$$\mathbf{A}_0 = \sqrt{M}\boldsymbol{\Lambda}_c\mathbf{C}(\mathbf{I} - \mathbf{J}), \quad \mathbf{A}_1 = -\sqrt{M}\boldsymbol{\Lambda}_c\mathbf{C}(\mathbf{I} + \mathbf{J}). \tag{8.5.16}$$

The set of M analysis filters can be expressed as in (8.5.1), where $\mathbf{e}(z)$ is the delay chain vector defined in (5.4.1). By using the above $\mathbf{A}_0$ and $\mathbf{A}_1$ we obtain

$$\mathbf{h}(z) = \sqrt{M}\boldsymbol{\Lambda}_c\mathbf{C}\,[\mathbf{I} - \mathbf{J} \quad -(\mathbf{I} + \mathbf{J})] \begin{bmatrix} \mathbf{g}_0(z^{2M}) & \mathbf{0} \\ \mathbf{0} & \mathbf{g}_1(z^{2M}) \end{bmatrix} \begin{bmatrix} \mathbf{e}(z) \\ z^{-M}\mathbf{e}(z) \end{bmatrix}. \tag{8.5.17}$$

Here $\mathbf{g}_i(z)$ are the diagonal matrices of polyphase components, defined as in (8.5.2). Using (8.5.17) we can draw the analysis bank as in Fig. 8.5-5(a). Fig. 8.5-5(b) shows the more explicit structure in terms of $G_k(z)$. (The decimators can be moved to the left as we did earlier in Fig. 8.3-2.)

Recall that the synthesis filters are given by $f_k(n) = h_k(N - n)$. From this we obtain the synthesis bank structure of Fig. 8.5-6, which the reader is requested to justify in Problem 8.10.

Fast implementation of the DCT. The DCT matrix $\mathbf{C}$ in the above figures can itself be implemented using fast techniques. A quick way to see this is to note that $\mathbf{C}$ can be embedded into the matrix $\mathbf{V}$ as shown in (8.4.4). This matrix can, in turn, be implemented as in Fig. 8.4-1. The main cost here is the implementaion of $\mathbf{W}^*$, where $\mathbf{W}$ is the DFT matrix. $\mathbf{W}^*$ can be implemented efficiently by use of the Fast Fourier Transform (FFT) [Oppenheim and Schafer, 1989]. For more efficient and direct 'fast DCT algorithms', see Yip and Rao [1987] and references therein.

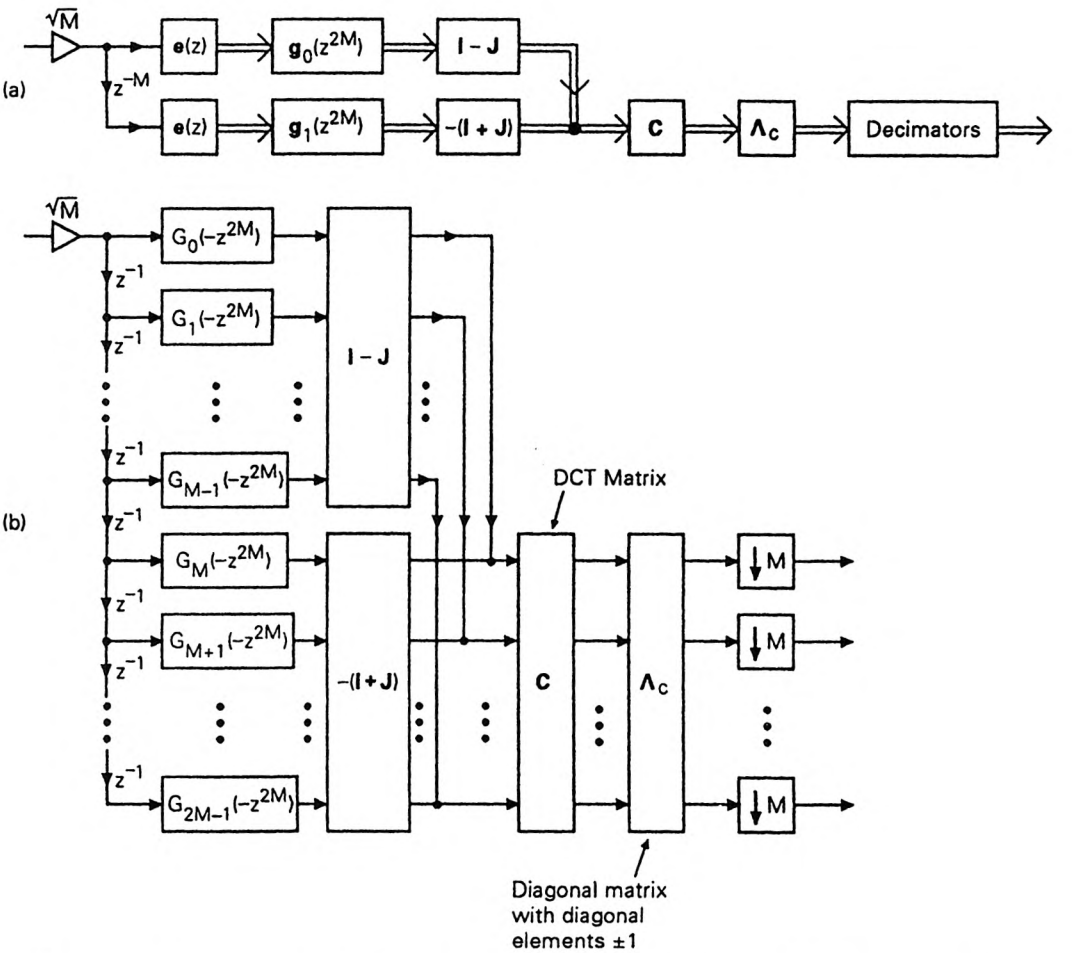

Figure 8.5-5 The cosine modulated analysis bank in terms of DCT. (a) Using matrix notations and (b) using more explicit notations. Here $N+1 = 2mM$, and m = even.

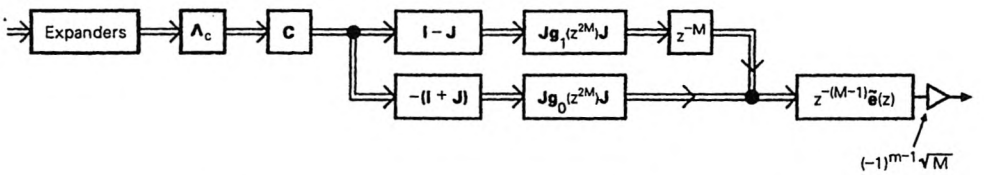

Figure 8.5-6 The cosine modulated synthesis bank, when $N+1 = 2mM$, with m = even.

8.5.5 Advantages of the Cosine Modulated PR System

We now summarize the advantages of the FIR cosine modulated perfect reconstruction system.

1. All analysis filters $H_k(z)$ are obtained from a real coefficient prototype $P_0(z)$, by cosine modulation as in (8.1.37). Only this prototype has to be optimized during the design, so that the design complexity is low. Due to the paraunitary constraint on the polyphase matrix, the number of parameters to be optimized is in fact only about half the number used in pseudo QMF design. Tables 8.5.1 and 8.5.2 give quantitative details.
2. With the synthesis filters chosen as $f_k(n) = h_k(N-n)$, we have perfect reconstruction. (In particular the analysis and synthesis filters have same order N). The objective function to be minimized during optimization of the coefficients of $P_0(z)$ is therefore very simple, and has to reflect only the stopband attenuation of $P_0(z)$.
3. If we optimize the lattice coefficients $\theta_{k,\ell}$ as in Sec. 8.5.2, then the paraunitary constraint is automatically imposed during the design of the prototype $P_0(z)$. So we can use an unconstrained optimization routine to compute $\theta_{k,\ell}$.
4. The *implementation* complexity for the entire analysis bank is equal to the cost of the prototype $P_0(z)$ plus the modulation cost (which depends on the number of channels M but not on the filter order N). This is same as that of the pseudo QMF system.
5. The modulation cost can be reduced by expressing the analysis and synthesis banks in terms of the DCT matrix (Figs. 8.5-5 and 8.5-6), for which there exist fast implementations.

Summarizing, the system has all the advantages and simplicity of the cosine modulated pseudo QMF system of Sec. 8.1, and in addition offers perfect reconstruction. The price paid for this is in terms of reduced stopband attenuation of the prototype $P_0(z)$, but this is a minor loss in practice (Table 8.5.3).

It should be emphasized that, even though the prototype filter has linear phase, the cosine modulated analysis filters do not, in general, have linear

phase. In fact, if we give up the linear phase property of the prototype, there are some advantages [Nguyen, 1992b]. Also see [Mau, 1992] for further generalizations.

PROBLEMS

8.1. In the pseudo QMF system discussed in Sec. 8.1 and 8.2, there is some residual aliasing distortion, which is measured by the quantity (8.2.10). Suppose we construct a new filter bank in which each $F_k(z)$ is interchanged with the corresponding $H_k(z)$. How is the measure (8.2.10) affected? How is the distortion function $T(z)$ affected?

8.2. For the pseudo QMF system we can find the synthesis filters either from (8.1.38) or from the relation $f_k(n) = h_k(N-n)$ where $h_k(n)$ is as in (8.1.37). Verify that these two yield the same synthesis filter coefficients.

8.3. Let $H_k(z)$ be a transfer function of the form

$$H_k(z) = \sum_{\ell=0}^{r-1} z^{-\ell} G_\ell(z^r) \cos(2\pi/r)(\ell + \ell_1)(k + k_0) \qquad (P8.3a)$$

where k_0 is a half-integer (i.e., $k_0 - 0.5$ is an integer) and ℓ_1 is arbitrary. Show that the impulse response of $H_k(z)$ has the form

$$h_k(n) = h(n) \cos(2\pi/r)(\ell_1 + n)(k + k_0), \qquad (P8.3b)$$

where $h(n)$ is the impulse response of $H(z)$, which is defined by

$$H(z) = \sum_{\ell=0}^{r-1} z^{-\ell} G_\ell(-z^r). \qquad (P8.3c)$$

8.4. Suppose we wish to design two-channel real coefficient FIR perfect reconstruction QMF banks using the method described in Sec. 8.5. Does this cover every design that can be generated using the two channel lattice structure of Sec. 6.4.3?

8.5. Consider the three types of FIR filter banks summarized in Sec. 8.5.3. Suppose $M = 15$ and filter lengths $N + 1 = 60$.

a) For each type, what is the number of parameters to be optimized during the design phase?

b) For each type, what are the number of MPUs and APUs required to implement the analysis bank?

8.6. Show that the DCT matrix $\mathbf{C}$ and DST matrix $\mathbf{S}$ are related as in (8.4.2).

8.7. Consider the expression inside the brackets in (8.4.7). Show that

$$\mathbf{\Lambda}_w^\dagger \mathbf{U}^\dagger \mathbf{\Lambda}_\beta^\dagger \mathbf{\Lambda}_\beta \mathbf{U} \mathbf{\Lambda}_w = 2M\mathbf{I}, \quad \text{and} \quad \mathbf{\Lambda}_w^\dagger \mathbf{U}^\dagger \mathbf{\Lambda}_\beta^\dagger \mathbf{J}_{2M} \mathbf{\Lambda}_\beta \mathbf{U} \mathbf{\Lambda}_w = 0. \qquad (P8.7)$$

Note. the second equality requires more work.

8.8. Assuming that the prototype satisfies the linear phase condition, $p_0(n) = p_0(N-n)$, establish the relation (8.5.8a) among the $2M$ polyphase components. (*Note.* $N + 1 = 2mM$.)

8.9. Let the $2M$ polyphase components of $P_0(z)$ satisfy (8.5.5) as well as (8.5.8a). Assuming $N+1 = 2mM$ and that M is odd, verify that

$$G_{\frac{M-1}{2}}(z) = \sqrt{0.5\alpha}z^{-K}, \quad \text{and} \quad G_{\frac{3M-1}{2}}(z) = \sqrt{0.5\alpha}z^{-(m-1-K)}. \qquad (P8.9)$$

Show further that K satisfies (8.5.15). You can use the fact that $P_0(z)$ is a linear phase lowpass filter with cutoff $\pi/2M$.

8.10. In the text we saw that the analysis bank represented by (8.5.17) can be implemented as in Fig. 8.5.5. Let the M synthesis filters be chosen as $f_k(n) = h_k(N-n)$. Then show that the synthesis filter bank can be realized as in Fig. 8.5-6. Also draw the structure more explicitly in terms of polyphase components (i.e., as we did in Fig. 8.5-5(b) for the analysis bank).

8.11. Let $P_0(z)$ be the FIR prototype described in Theorem 8.5.1. Let the polyphase components of this prototype satisfy (8.5.5). Show then that $\widetilde{P}_0(z)P_0(z)$ is a Nyquist($2M$) filter.